

OAK RIDGE  
NATIONAL LABORATORY

MANAGED BY UT-BATTELLE  
FOR THE DEPARTMENT OF ENERGY

Prepared by



ORNL-27 (4-00)

## DOCUMENT AVAILABILITY

Reports produced after January 1, 1996, are generally available free via the U.S. Department of Energy (DOE) Information Bridge:

**Web site:** <http://www.osti.gov/bridge>

Reports produced before January 1, 1996, may be purchased by members of the public from the following source:

National Technical Information Service  
5285 Port Royal Road  
Springfield, VA 22161  
**Telephone:** 703-605-6000 (1-800-553-6847)  
**TDD:** 703-487-4639  
**Fax:** 703-605-6900  
**E-mail:** [info@ntis.fedworld.gov](mailto:info@ntis.fedworld.gov)  
**Web site:** <http://www.ntis.gov/support/ordernowabout.htm>

Reports are available to DOE employees, DOE contractors, Energy Technology Data Exchange (ETDE) representatives, and International Nuclear Information System (INIS) representatives from the following source:

Office of Scientific and Technical Information  
P.O. Box 62  
Oak Ridge, TN 37831  
**Telephone:** 865-576-8401  
**Fax:** 865-576-5728  
**E-mail:** [reports@adonis.osti.gov](mailto:reports@adonis.osti.gov)  
**Web site:** <http://www.osti.gov/contact.html>

This report was prepared as an account of work sponsored by an agency of the United States Government. Neither the United States government nor any agency thereof, nor any of their employees, makes any warranty, express or implied, or assumes any legal liability or responsibility for the accuracy, completeness, or usefulness of any information, apparatus, product, or process disclosed, or represents that its use would not infringe privately owned rights. Reference herein to any specific commercial product, process, or service by trade name, trademark, manufacturer, or otherwise, does not necessarily constitute or imply its endorsement, recommendation, or favoring by the United States Government or any agency thereof. The views and opinions of authors expressed herein do not necessarily state or reflect those of the United States Government or any agency thereof.

## **Nuclear Science and Technology Division**

Prepared by the  
OAK RIDGE NATIONAL LABORATORY  
P.O. Box 2008  
Oak Ridge, Tennessee 37831-6285  
managed by  
UT-BATTELLE, LLC  
for the  
U.S. DEPARTMENT OF ENERGY  
under contract DE-AC05-00OR22725

# Contents

<b>List of Figures</b> .....	v
<b>List of Tables</b> .....	vi
<b>Abstract</b> .....	1
<b>I. Introduction</b> .....	1
<b>II. Cross Section Data</b> .....	1
<b>III. Resonance Analysis and Results</b> .....	2
A. Total Cross Section Analysis .....	4
1. ORELA Transmission Data .....	4
2. Cierjacks, et al. Data .....	5
3. Brugger, et al. Data .....	5
4. Singh, et al. Data .....	7
B. (n,p) Cross Section Analysis .....	8
C. Capture Cross Section Analysis .....	11
D. Thermal and Integral Quantities .....	12
E. Individual Resonance Discussion .....	13
F. Comparison with ENDF/B-VI .....	14
G. Level Statistics .....	16
<b>IV. Summary and Conclusions</b> .....	18
<b>V. Acknowledgments</b> .....	18
<b>References</b> .....	19

## List of Figures

1	Comparison of SAMMY fits (solid lines) to the $^{nat}\text{Cl}$ total cross section data of Brugger, et al. [7] (+ symbols) and Guber, et al. [2] (open circles); the $^{nat}\text{Cl}$ capture data of Kashukeev, et al. [10] (open squares); and the $^{35}\text{Cl}(\text{n},\text{p})$ data of Koehler [11] (solid circles). The x symbols denote the ENDF/B-VI thermal values.	3
2	Comparison of SAMMY fits (solid lines) to the $^{nat}\text{Cl}$ transmission data of Guber, et al. [2] for $0 < E_n < 500$ keV.	4
3	Comparison of SAMMY fits (solid lines) to the $^{nat}\text{Cl}$ total cross section data of Cierjacks, et al. [5] (KFK) and Guber, et al. [2] (ORELA) for $500 < E_n < 850$ keV.	5
4	Comparison of SAMMY fits (solid lines) to the $^{nat}\text{Cl}$ total cross section data of Cierjacks, et al. [5] (KFK) and Guber, et al. [2] (ORELA) for $850 < E_n < 1200$ keV.	6
5	Comparison of SAMMY fits (solid line) to the $^{nat}\text{Cl}$ total cross section data of Brugger, et al. [7] (+ symbols) and Guber, et al. [2] (open circles). The ENDF/B-VI thermal value is shown as an x.	7
6	Comparison of SAMMY fits (solid line) to the $^{nat}\text{Cl}$ total cross section data of Singh, et al. [6] for $4 < E_n < 400$ keV.	8
7	Comparison of SAMMY fits (solid line) to the $^{35}\text{Cl}(\text{n},\text{p})$ cross section data of Koehler [11] for $0.025 \text{ eV} < E_n < 10 \text{ keV}$ .	10
8	Comparison of SAMMY fits (solid line) to the $^{35}\text{Cl}(\text{n},\text{p})$ cross section data of Druyts, et al. [12] for selected resonances.	10
9	Comparison of SAMMY fits (solid line) to the $^{nat}\text{Cl}$ capture cross section data of Guber, et al. [2] for $14 < E_n < 500$ keV.	11
10	Comparison of SAMMY fits (solid line) to the $^{nat}\text{Cl}$ capture and transmission data of Guber, et al. [2], the transmission data of Good, et al. [4], the $^{35}\text{Cl}(\text{n},\text{p})$ data of Druyts, et al. [12], and the total cross section data of Singh, et al. [6] for resonances at 398 and 4251 eV.	14
11	Comparison of $^{35}\text{Cl}$ total cross sections from ENDF/B-VI and the present evaluation.	15
12	Comparison of the neutron width distribution with the Porter-Thomas distribution for $J = 2$ , s-wave $^{35}\text{Cl}$ resonances.	16
13	Comparison of the level spacing distribution with the Wigner distribution for $J = 2$ , s-wave $^{35}\text{Cl}$ resonances.	17

## List of Tables

I	Data Sets for $^{35,37,nat}\text{Cl}$ Evaluation . . . . .	2
II	Proton Widths and Resonance Strengths $\omega = g\Gamma_n\Gamma_p/\Gamma$ for $^{35}\text{Cl}(n,p)$ from the present evaluation compared with the data of Druyts, et al. [12], Koehler [11], and Gledenov [19]. The results are normalized to a thermal cross section of 483 mb. . . . .	9
III	Cl Thermal Cross Sections and Resonance Integrals for T = 0K . . . . .	13
IV	Energies and Widths for Resonances in $^{35}\text{Cl}(n,X)$ . . . . .	20
V	Energies and Widths for Resonances in $^{37}\text{Cl}(n,X)$ . . . . .	27

## ABSTRACT

We have performed an evaluation of  $^{35}\text{Cl}$ ,  $^{37}\text{Cl}$ , and  $^{nat}\text{Cl}$  neutron cross sections in the resolved resonance region with the multilevel Reich-Moore R-matrix formalism. Resonance analyses were carried out with the computer code SAMMY, which utilizes Bayes' method, a generalized least squares technique. A recent modification of SAMMY enabled us to calculate charged particle penetrabilities for the proton exit channel. Our resonance parameter representation describes the data much better than does ENDF/B-VI, and it should lead to improved criticality safety calculations for systems where Cl is present.

## I. INTRODUCTION

Existing evaluated nuclear data have been obtained primarily for applications to thermal and fast reactors, and to fusion systems. In contrast to these systems, typical neutron spectra in criticality safety applications peak in the epithermal energy range. For many important elements the existing evaluations or the underlying nuclear data are not sufficiently accurate for reliable calculation of criticality safety margins; consequently, improved measurements and evaluations are needed for these elements.

Chlorine is an important element in criticality safety applications where chlorides are present in significant amounts; for example, polyvinyl chloride pipe is 57% Cl by weight. Several deficiencies in the existing ENDF/B-VI data evaluation [1] for Cl have been discussed previously [2]. In this paper we describe a resonance parameter evaluation of  $^{35}\text{Cl}$ ,  $^{37}\text{Cl}$ , and  $^{nat}\text{Cl}$  neutron cross sections in the resolved resonance region with the multilevel Reich-Moore R-matrix formalism using the code SAMMY [3]. Our evaluation takes advantage of recent high-resolution capture and transmission measurements at the Oak Ridge Electron Linear Accelerator (ORELA) to extend the resolved resonance energy range to 1.2 MeV with much more accurate representation of the data than previous evaluations. In the following sections we discuss the cross section data, resonance analysis, results, and conclusions.

## II. CROSS SECTION DATA

Standard nuclear databases and the open literature were searched for capture, total, and reaction cross section data sets. Selected information about the data sets used in our analysis is listed in Table I.

The total cross section data include measurements by Guber, et al. [2] and Good, et al. [4], on the 80-m flight path at ORELA; Cierjacks, et al. [5], on a 57-m flight path at the Karlsruhe Isochronous Cyclotron; Singh, et al. [6] on the 200-m flight path at the Columbia synchrocyclotron; Brugger, et al. [7], who utilized a crystal spectrometer and also the MTR fast chopper with a flight path of 45 m; Kiehn, et al. [8], with the Rockefeller generator; and Newson, et al. [9], at the Duke Van de Graaff facility. The Cierjacks data were normalized to the data of Guber, et al. by integrating over the energy range 500 to 1200 keV. The normalization factor was 1.054. A neutron energy transformation was applied to the Cierjacks data to make the peak energies consistent with the corresponding ORELA values.

TABLE I: Data Sets for  $^{35,37,nat}\text{Cl}$  Evaluation

Data Type	Authors	Facility	Flight Path (m)	Energy Range (keV)	Analysis	Atoms/barn
Transmission	Guber, et al.[2]	ORELA	79.82	0.02	-	1250 0.207
Transmission	Good, et al.[4]	ORELA	78.20	0.38	-	0.42 0.0081
Total	Singh, et al.[6]	Columbia cyclotron	202.05	0.02	-	400 0.198
Total	Brugger, et al.[7]	MTR fast chopper	45	0.03	-	15 0.036
Total	Cierjacks, et al.[5] <sup>a</sup>	KFK cyclotron	57.54	500	-	1250 0.262
Total	Kiehn, et al.[8]	Rockefeller generator		133	-	1084
Total	Newson, et al.[9]	Duke Van de Graaff		7	-	194 0.057
Capture	Guber, et al.[2]	ORELA	40	0.1	-	500 0.098
Capture	Kashukeev, et al.[10]			0.022	-	1
$^{35}\text{Cl}(\text{n},\text{p})$	Koehler[11]	LANSCE		thermal	-	35
$^{35}\text{Cl}(\text{n},\text{p})$	Druyts, et al.[12]	GELINA	8, 30	0.3	-	110

<sup>a</sup>Normalization factor of 1.054, relative to data of Guber, et al, was obtained by integrating the total cross section from 500 to 1250 keV.

Also included in the evaluation were the high resolution capture cross section data ( $0.1 < E_n < 500$  keV) of Guber, et al. [2] and the older, low resolution capture data ( $0.02 < E_n < 1.0$  keV) of Kashukeev, et al. [10]. The  $^{35}\text{Cl}(\text{n},\text{p})^{35}\text{S}$  cross section data of Koehler [11] and Druyts, et al. [12] were also fit and included in the evaluation. The proton widths are significant fractions of the total widths for resonances at 398 and 4251 eV.

### III. RESONANCE ANALYSIS AND RESULTS

Resonance parameters were determined by a consistent analysis in which corrections for Doppler broadening, resolution broadening, multiple scattering, and other experimental effects were incorporated. Data sets were analyzed sequentially so that each fit was connected to the previous fit by the SAMMY parameter covariance matrix, thereby yielding energies and widths for 67 s-wave and 319 p-wave resonances in the range  $0.2 < E_n < 1200$  keV. Of these 386 s- and p-wave resonances, 248 were assigned to  $^{35}\text{Cl}$  and 138 to  $^{37}\text{Cl}$ . Two negative-energy resonances were included to account for bound levels and several high-energy resonances were included to account for the effect of resonances above 1200 keV. Fits were obtained for recent ORELA transmission and capture data [2] as well as for several older, EXFOR cross section data sets.

In order to give a proper treatment for charged particles in an exit channel, an algorithm to calculate charged particle penetrabilities (CPP) and shifts was incorporated in the SAMMY code. The methodology for CPP computation has been given previously [13]. Routines based on the CPP algorithm have been developed and incorporated in a development version of the nuclear data processing code NJOY [14] for use in preparing data for criticality safety benchmark calculations.

The nuclear radii used for penetrabilities and shifts were computed according to  $R = 1.23A^{1/3} + 0.8$  fm, where A is the nuclide mass. These values were 4.8222 and 4.8974 fm for

$^{35}\text{Cl}$  and  $^{37}\text{Cl}$ , respectively. In the SAMMY analysis the radii used to compute hard sphere phase shifts were allowed to vary, and different radii were allowed for s- and p-waves. Final values for  $^{35}\text{Cl}$  were  $R(l=0,1) = 3.6680, 4.8888 \text{ fm}$ ; final values for  $^{37}\text{Cl}$  were  $R(l=0,1) = 3.3651, 3.9565 \text{ fm}$ .

For  $E_n < 1 \text{ keV}$ , Fig. 1 shows a global view of the final SAMMY fits to the total cross section values of Refs. [2, 7], the  $^{35}\text{Cl}(n,p)$  cross section values of Ref. [11], and the low resolution capture data of Ref. [10]. Also shown are the thermal values from ENDF/B-VI.

R. O. Sayer ORNL 23 Sep 2002

CLnat\_tot\_GU01\_BR56\_020502.KG4

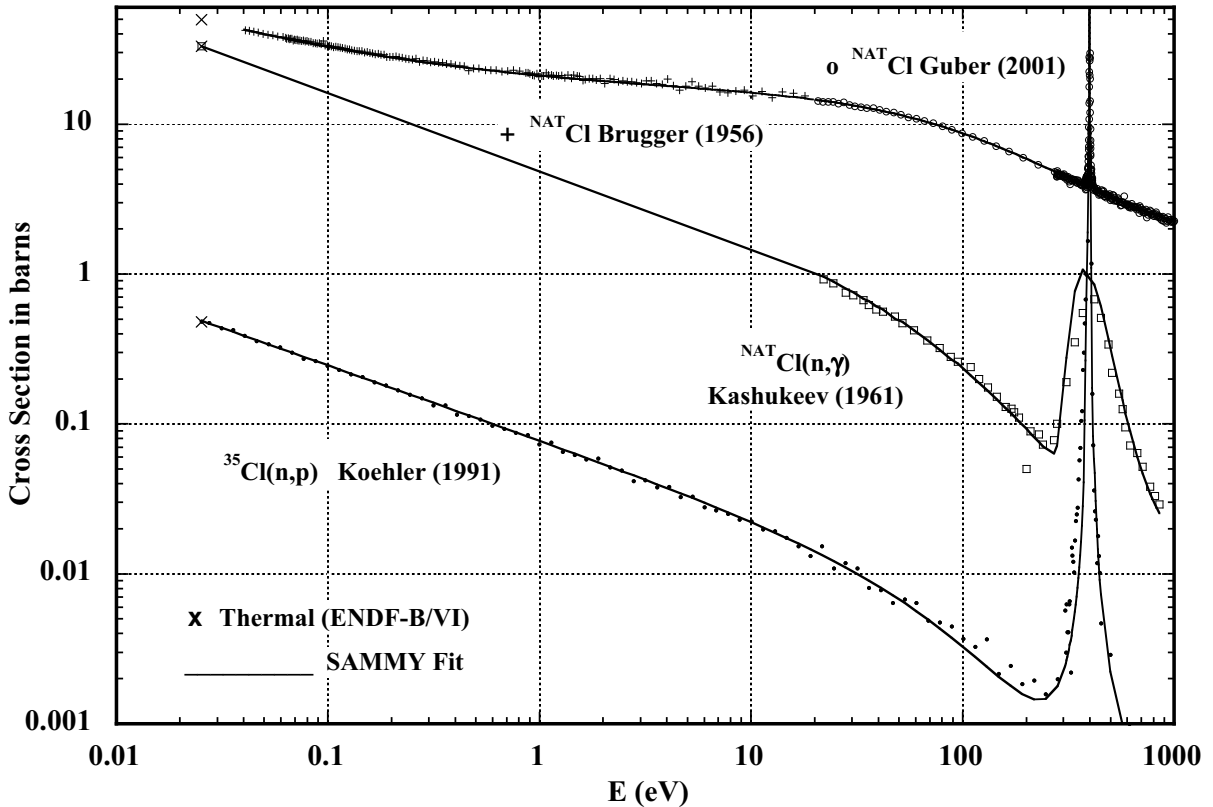


FIG. 1: Comparison of SAMMY fits (solid lines) to the  $^{nat}\text{Cl}$  total cross section data of Brugger, et al. [7] (+ symbols) and Guber, et al. [2] (open circles); the  $^{nat}\text{Cl}$  capture data of Kashukeev, et al. [10] (open squares); and the  $^{35}\text{Cl}(n,p)$  data of Koehler [11] (solid circles). The x symbols denote the ENDF/B-VI thermal values.

Below the first resonance at 398 eV, the magnitude and shape of the cross section is determined by the  $^{35}\text{Cl}(n,p)$  data of Ref. [11], the total cross section data of Ref. [7], the transmission data of Ref. [2], and the well-known thermal values [15]. These data were analyzed sequentially to obtain parameters for the -180 eV bound state. This analysis resulted in a renormalization of the data of Ref. [7] by a factor of 0.992.

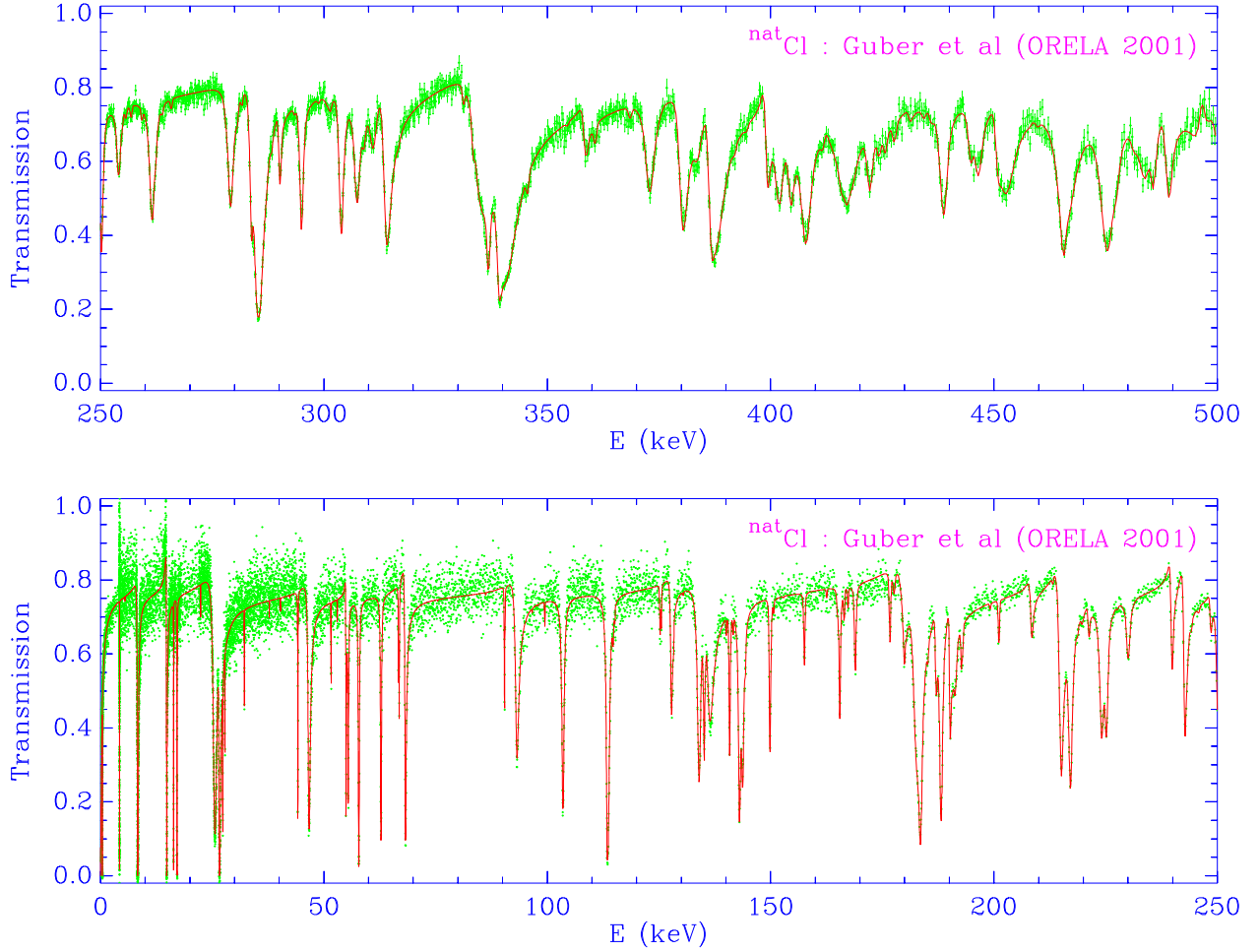


FIG. 2: Comparison of SAMMY fits (solid lines) to the  $^{nat}\text{Cl}$  transmission data of Guber, et al. [2] for  $0 < E_n < 500$  keV.

## A. Total Cross Section Analysis

### 1. ORELA Transmission Data

Guber, et al. [2] measured the transmission of a natural  $\text{CCl}_4$  sample (thickness for Cl 0.2075 atoms/b) over the range  $0.020 < E_n < 1500$  keV, using the 80-m flight path at ORELA. These data exhibit much higher energy resolution and lower background than the older data sets included in our evaluation. This high resolution is shown in Fig. 2, where the SAMMY fits are compared with the transmission data for  $0 < E_n < 500$  keV. Since this sample was too thick to give an accurate neutron width for the 398 eV resonance, we also fit the transmission data of Good, et al. [4] who used a sample of thickness 0.00812 atoms/b.

## 2. Cierjacks, et al. Data

Cierjacks, et al. [5] measured total cross sections for  $500 < E_n < 1250$  keV, using a 57-m flight path at the Karlsruhe Isochronous Cyclotron. A natural  $\text{CCl}_4$  sample of thickness 0.262 atoms/b and chemical purity 99% was utilized. The Cierjacks data were normalized to the data of Guber, et al. [2], by integrating over the energy range 500 to 1200 keV. The normalization factor was 1.054. A neutron energy transformation was applied to the Cierjacks data to make the peak energies consistent with the corresponding ORELA values. Examples of SAMMY fits to the Cierjacks data and the Guber data are presented in Figs. 3 and 4. The Cierjacks data and fit were shifted upwards for display purposes.

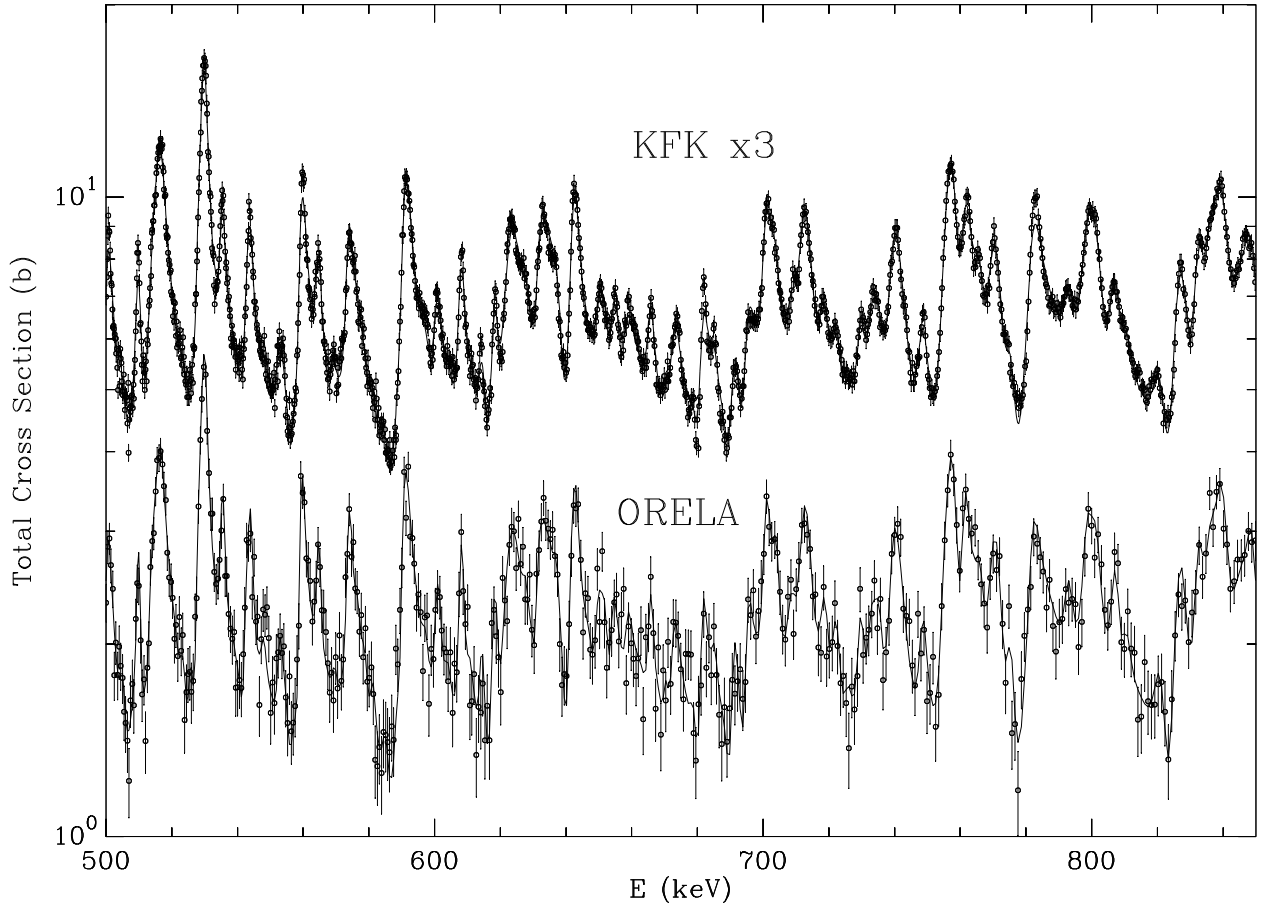


FIG. 3: Comparison of SAMMY fits (solid lines) to the  $^{nat}\text{Cl}$  total cross section data of Cierjacks, et al. [5] (KFK) and Guber, et al. [2] (ORELA) for  $500 < E_n < 850$  keV.

## 3. Brugger, et al. Data

Brugger, et al. [7] utilized the MTR fast chopper with a flight path of 45 m to measure transmission values over the range 16 eV to 15 keV. They also used the MTR crystal spectrometer for measurements over the range 0.03 to 70 eV. A  $\text{CCl}_4$  sample of thickness 2.115 g/cm<sup>2</sup> was used with the MTR crystal spectrometer;  $\text{CCl}_4$  and  $\text{NaCl}$  samples were used

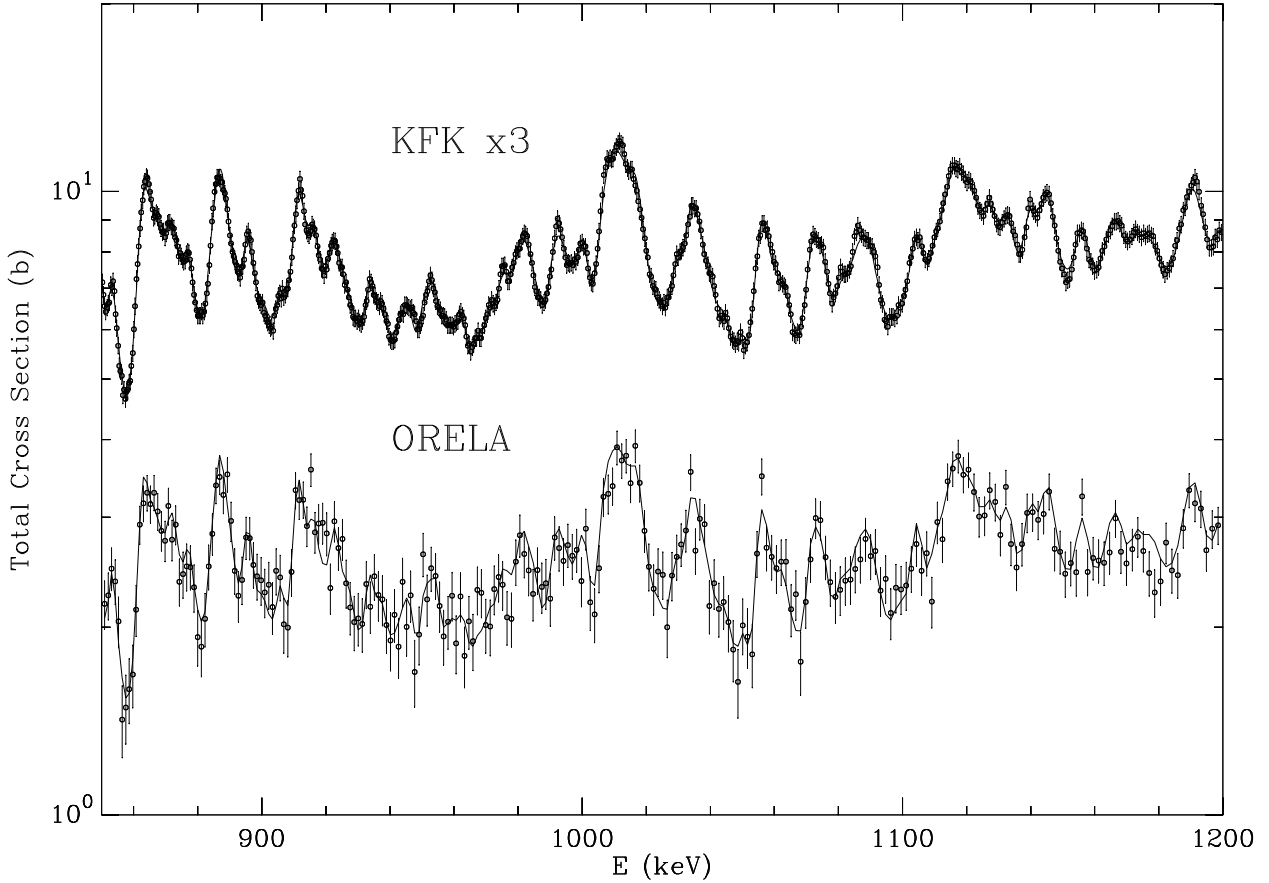


FIG. 4: Comparison of SAMMY fits (solid lines) to the  $^{nat}\text{Cl}$  total cross section data of Cierjacks, et al. [5] (KFK) and Guber, et al. [2] (ORELA) for  $850 < E_n < 1200$  keV.

with the MTR fast chopper. Fig. 5 shows a comparison of  $\sigma_{total}$  values computed from our resonance parameters with the data of Brugger, et al. and Guber, et al. for  $0.01 \text{ eV} < E_n < 1 \text{ keV}$ . The higher precision ORELA data, which begin at 20 eV, determine the fit above 20 eV. Brugger, et al. state that their measurement precision is very good up to 10 eV, and our calculated values agree with the Brugger data (average of 6 points) to better than 2% for  $0.04 < E_n < 3 \text{ eV}$ .

Near 0.03 eV, the cross section computed from our resonance parameter representation and the fit by Brugger, et al. are about 3% higher than the Brugger data. We note that Brugger, et al. did not correct their data for second order effects in the monochromating crystal; this correction would increase the experimental values at the lowest energies and produce better agreement with the predicted values. Extrapolation of the Brugger data from 0.03 to 0.0253 eV gives a thermal cross section of about 47 b, a value significantly lower than the ENDF/B-VI value of 49.6 b ( $T = 300\text{K}$ ). As shown in Fig. 5, our predicted thermal  $\sigma_{total}$  value is in excellent agreement with the ENDF/B-VI value. As previously noted, the SAMMY sequential analysis produced a normalization of 0.992 for the Brugger, et al. [7] data.

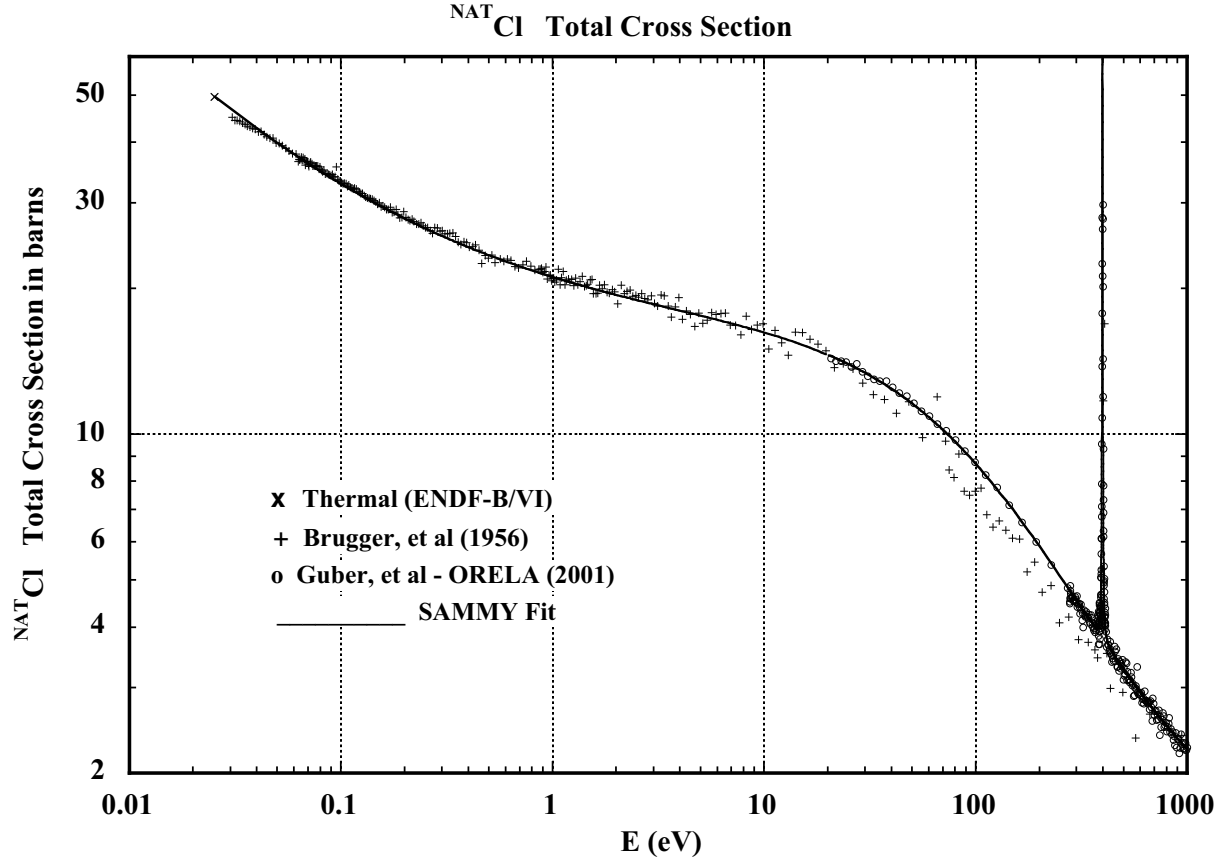


FIG. 5: Comparison of SAMMY fits (solid line) to the  $^{nat}\text{Cl}$  total cross section data of Brugger, et al. [7] (+ symbols) and Guber, et al. [2] (open circles). The ENDF/B-VI thermal value is shown as an x.

#### 4. Singh, et al. Data

Singh, et al. [6] used the 200-m flight path at the Columbia synchrocyclotron to measure transmissions and determine total cross sections for  $^{nat}\text{Cl}$  for samples of thickness 0.198, 0.307, and 0.00764 atoms/b over the energy range 0.02 to 400 keV. The authors state that their background determination is rather uncertain for  $E > 100$  keV, and that below 100 eV they adjusted their background values to fit the data of Brugger, et al. [7] near 20 and 100 eV. For several energy ranges (0.03-1 keV; 115-180 keV; 205-400 keV) the Singh data differ from the more recent, high resolution ORELA data [2] by 10 to 20%. Consequently, we de-emphasized the regions between resonances by averaging the Singh data and assigning large uncertainties.

Doppler and resolution broadening were taken into account in the fits. Since no uncertainties were quoted for the EXFOR data set, values of 10% were assigned near resonances, and the normalization was varied in the analysis. Results of the SAMMY fits are shown in Fig. 6.

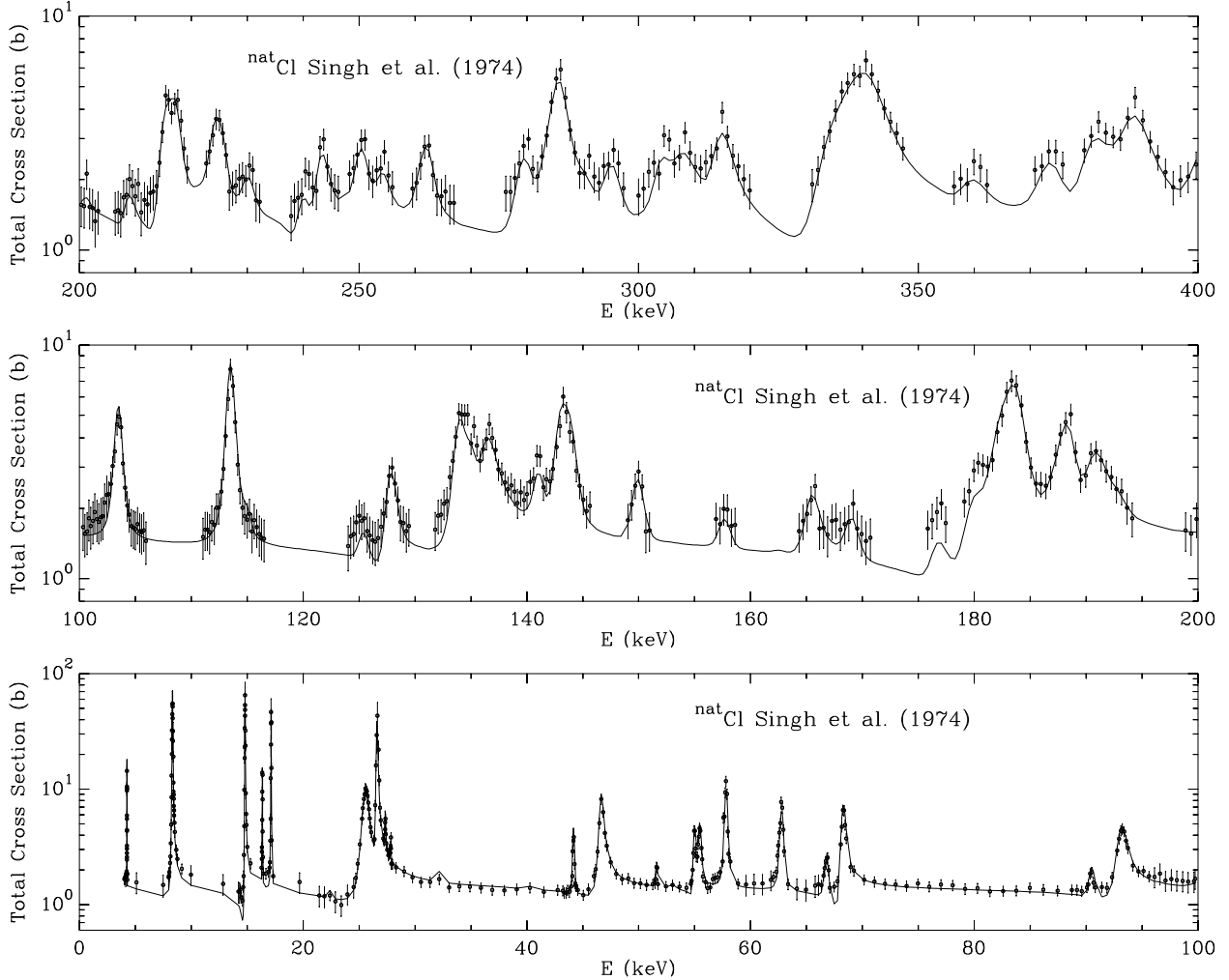


FIG. 6: Comparison of SAMMY fits (solid line) to the  $^{nat}\text{Cl}$  total cross section data of Singh, et al. [6] for  $4 < E_n < 400$  keV.

### B. (n,p) Cross Section Analysis

The  $^{35}\text{Cl}(n,p)^{35}\text{S}$  data of Koehler [11] and Druyts, et al. [12] were analyzed with the SAMMY code, which has been modified to compute charged particle penetrabilities. The Q value for the  $^{35}\text{Cl}(n,p)^{35}\text{S}$  reaction is +0.61522 MeV.

A wide range of  $^{35}\text{Cl}(n,p)$  thermal cross section values has been reported [15] from both activation and proton-emission experiments. In 1991 Koehler chose to normalize his data to the most accurate value then available,  $489 \pm 14$  mb, measured by Sims and Juhnke [16] and recommended by Mughabghab, et al. [15]. Sims and Juhnke made activation measurements relative to a  $^{59}\text{Co}$  thermal cross section of 37.5 b. With the more recent value [15] for  $^{59}\text{Co}$ , 37.18 b, and a  $^{35}\text{Cl}$  abundance of 0.7577, we obtain  $483 \pm 14$  mb for the  $^{35}\text{Cl}(n,p)$  thermal cross section.

More recently (1994) Druyts, et al. [12] observed protons emitted from AgCl samples exposed to thermal neutrons from the ILL (Grenoble) High Flux Reactor. They report a cross section of  $440 \pm 10$  mb, which is significantly lower than the best activation value. However, an earlier proton-emission measurement by Schroder, et al. [17] gave a thermal

cross section of  $466 \pm 40$  mb, a value based on  $\sigma_{thermal} = 4.30 \pm 0.34$  b for  $^{40}\text{K}(n,p_0)$ . Furthermore, Gledenov, et al. [18] recently reported a much larger value,  $575 \pm 13$  mb, for the  $^{35}\text{Cl}(n,p)$  thermal cross section.

In the  $^{35}\text{Cl}(n,p)$  analysis we tried data normalizations that corresponded to varying the thermal (n,p) cross section from 440 to 483 mb. For resonances at 0.398 and 4.251 keV,  $\Gamma_p$  is a significant fraction of the total width, hence  $\sigma_{total}$  and  $\sigma_\gamma$  are sensitive to  $\Gamma_p$ . In addition  $\Gamma_p$  depends on the resonance strengths  $g\Gamma_n\Gamma_p/\Gamma$  deduced by Koehler [11] and Druyts, et al. [12] from area analysis of their peaks. Thus,  $\Gamma_p$  and normalization values must give resonance strengths consistent with experimental peak areas as well as satisfactory fits to the transmission, capture, and  $^{35}\text{Cl}(n,p)$  data. We could not find acceptable fits to all the data with a normalization significantly lower than  $\sigma_{thermal} = 483$  mb.

Proton, neutron, and capture widths used in our evaluation are given in Table II for resonances seen in the  $^{35}\text{Cl}(n,p)$  data. Resonance strengths  $\omega = g\Gamma_n\Gamma_p/\Gamma$  from our evaluation are compared with corresponding values of Koehler, Druyts, et al., and Gledenov, et al. [19]. For  $E \geq 14.8$  keV, the  $\Gamma_p$  values were computed from the  $\omega$  values of Druyts, et al. All values in Table II are normalized to  $\sigma_{thermal} = 483$  mb.

TABLE II: Proton Widths and Resonance Strengths  $\omega = g\Gamma_n\Gamma_p/\Gamma$  for  $^{35}\text{Cl}(n,p)$  from the present evaluation compared with the data of Druyts, et al. [12], Koehler [11], and Gledenov [19]. The results are normalized to a thermal cross section of 483 mb.

E (eV)	J	$\Gamma_\gamma$ (meV)	$\Gamma_n$ (meV)	$\Gamma_p$ (meV)	$\omega$ (meV)	$\omega$ [Druyts] (meV)	$\omega$ [Koehler] (meV)	$\omega$ [Gledenov] (meV)
397.8	2	665	50.5	322	9.8	9 ± 1	10	10.8 ± 1.6
4250.8	1	472	628	230	40.8	42 ± 3	35	40.0 ± 8.0
14801.9	2	346	32600	28	17	18 ± 5		
16356.1	(3)	386	5982	164	131	131 ± 16	64	
17133.9	3	802	14096	32	26	26 ± 9		
27346.4	(2)	458	6028	147	83	82 ± 22	69	
51608.0	(3)	45	2417	96	79	79 ± 40		
57811.6	(2)	538	107389	998	615	615 ± 121	860	
90420.2	(2)	716	21788	274	164	165 ± 66		
103515.4	1	388	381952	1973	735	735 ± 263		

For  $E \geq 14.8$  keV, the  $\Gamma_p$  values were computed from the  $\omega$  values of Druyts, et al. [12].

SAMMY fits are compared with the data of Koehler and Druyts, et al. in Figs. 7 and 8, respectively. Between resonance peaks, the Druyts, et al. data were very uncertain, and therefore only the peak regions were included in our analysis.

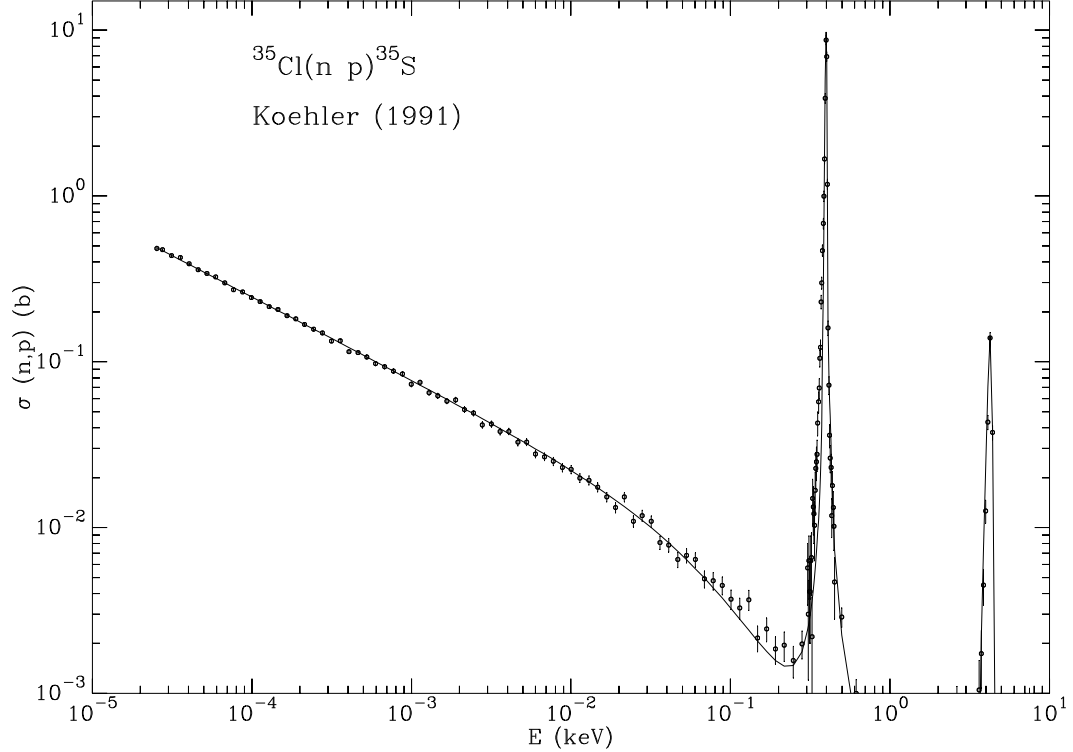


FIG. 7: Comparison of SAMMY fits (solid line) to the  $^{35}\text{Cl}$  ( $\text{n},\text{p}$ ) cross section data of Koehler [11] for  $0.025 \text{ eV} < E_n < 10 \text{ keV}$ .

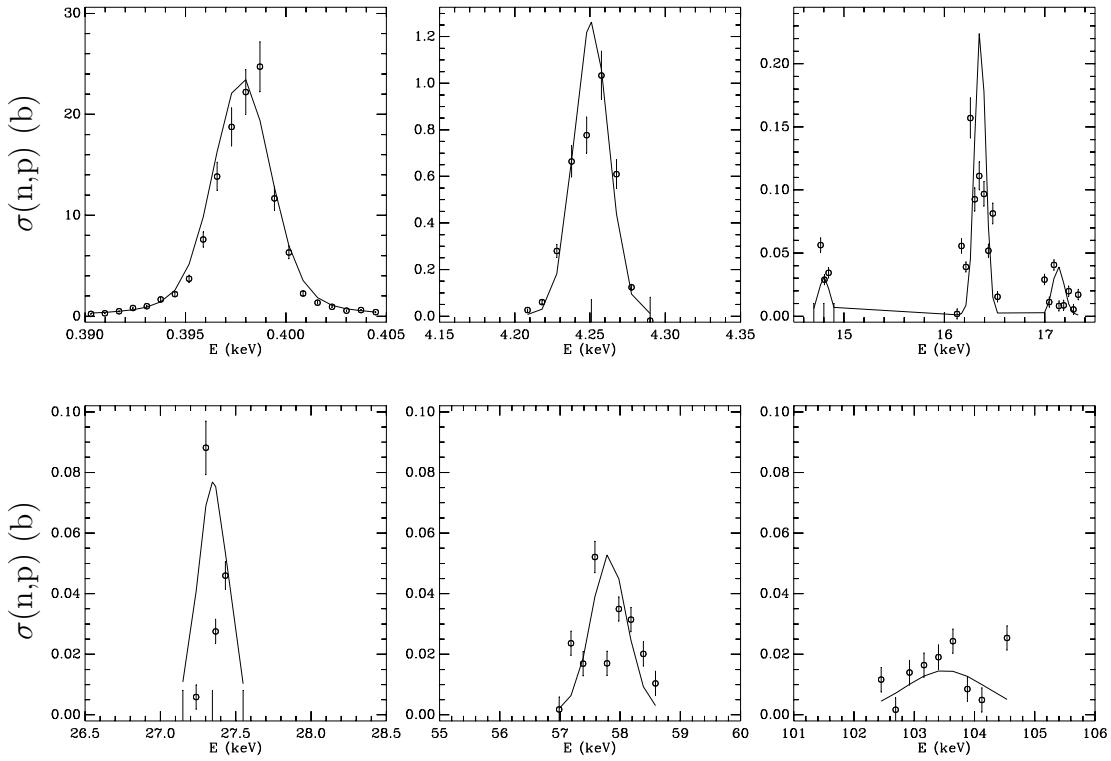


FIG. 8: Comparison of SAMMY fits (solid line) to the  $^{35}\text{Cl}$  ( $\text{n},\text{p}$ ) cross section data of Druyts, et al. [12] for selected resonances.

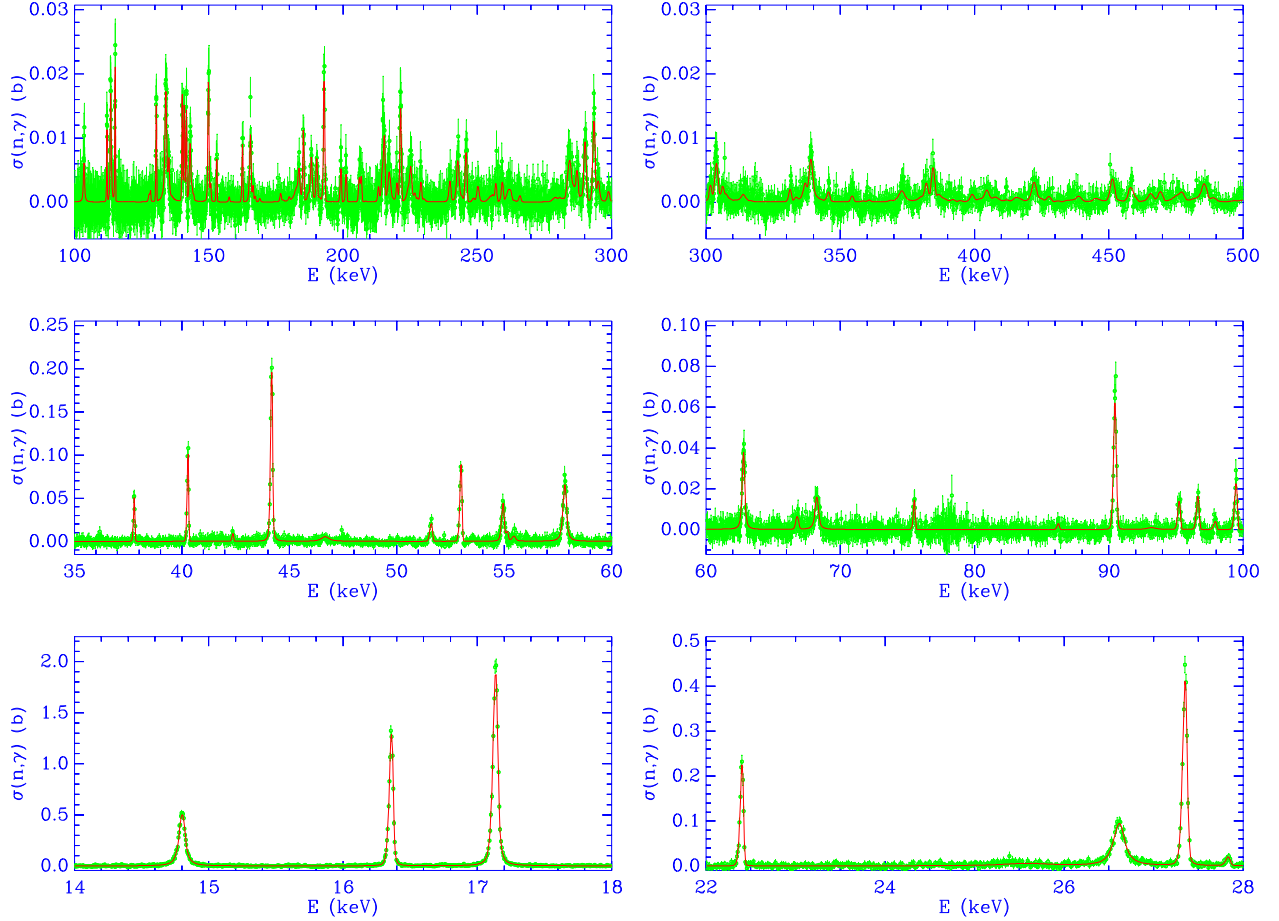


FIG. 9: Comparison of SAMMY fits (solid line) to the  $^{nat}\text{Cl}$  capture cross section data of Guber, et al. [2] for  $14 < E_n < 500$  keV.

### C. Capture Cross Section Analysis

Guber, et al. [2] measured the neutron capture of chlorine up to 500 keV using a natural LiCl sample of thickness 0.09812 atoms/b and the ORELA capture system, which had been re-engineered [20] to minimize the amount of structural material surrounding the sample and detectors. To calculate accurate correction factors for experimental effects of the neutron capture data, reliable neutron widths are needed since the sample was fairly thick. Initial  $\Gamma_n$  values were obtained by fitting the transmission data; using these newly determined  $\Gamma_n$  values, corrections for self-shielding and multiple scattering were calculated with SAMMY and used to determine capture widths. Several iterations of fitting the transmission and capture data were performed to obtain final resonance parameters for  $0.1 < E_n < 500$  keV.

From their resonance parameters, Guber, et al. [2], calculated average cross sections that were rather different from ENDF/B-VI. This difference is very likely the result of underestimated neutron sensitivity in the older measurements as well as an improved calculation of the weighting function.

In Fig. 9 we compare the capture cross section computed from our resonance parameters with the data of Guber, et al. [2]. Except in the resonance peaks, the calculation is generally hidden under the data points.

In nuclides where the  $(n, \gamma)$  cross section is small, the direct capture (DC) is often a significant fraction of the cross section. Guber, et al. [2] describe in detail the DC calculations they performed for  $^{35}\text{Cl}$  and  $^{37}\text{Cl}$  using the code TEDCA [21, 22]. They calculated that the effect of the DC component was very small for  $^{35}\text{Cl}$  where the thermal capture cross section is 43.6 b. However, for  $^{37}\text{Cl}$  approximately 0.31 b of the thermal capture cross section of 0.433 b is due to direct capture. The parameterized results obtained for the DC for  $^{35,37}\text{Cl}$  are given as follows with the cross section in mb and the neutron energy in keV:

$$\sigma_{DC}(^{35}\text{Cl}) = \frac{0.792 \pm 0.238}{\sqrt{E}} (1 + 2.83 \times 10^{-3} E + 2.22 \times 10^{-4} E^2) \quad E < 10 \text{ keV}$$

$$\sigma_{DC}(^{37}\text{Cl}) = \frac{1.549 \pm 0.811}{\sqrt{E}} (1 + 1.57 \times 10^{-6} E + 4.53 \times 10^{-7} E^2) \quad E < 100 \text{ keV}$$

The  $^{35}\text{Cl}$  ( $^{37}\text{Cl}$ ) formulas are estimated to be valid up to 10 (100) keV. Up to these energy limits the DC cross section for Cl varies nearly as  $1/v$ . The calculated  $^{35}\text{Cl}$  DC cross section at 10 keV is  $0.26 \pm 0.08$  mb, and the calculated  $^{37}\text{Cl}$  DC cross section at 100 keV is  $0.16 \pm 0.08$  mb. At these upper energy limits the computed DC values are larger than  $1/v$  by 5% for  $^{35}\text{Cl}$  and by 0.5% for  $^{37}\text{Cl}$ . At higher energies the DC part is expected to fall off more quickly than  $1/v$  because more and more flux is going into the resonant compound channel. In the DC calculation this would lead to an imaginary part of the optical neutron potential which increases with energy. However, such an imaginary potential was not considered because the energy-dependence is poorly constrained. It can be safely assumed that the DC contribution is negligible about 10 keV (or a few tens of keV) above the given upper limit.

In order to calculate astrophysical  $(n, \gamma)$  rates, Guber, et al. [2] adjusted their resonance parameters to account for the influence of direct capture. In this paper, we have deduced a set of resonance parameters, including the external level parameters, that reproduce the resonant part of the capture cross section. To this resonant part, one must add the DC contribution to obtain the overall capture cross section. The thermal value of the DC cross section is  $0.16 \pm 0.05$  b for  $^{35}\text{Cl}$  and  $0.31 \pm 0.16$  b for  $^{37}\text{Cl}$ .

#### D. Thermal and Integral Quantities

Table III gives a comparison of our elastic, capture,  $(n,p)$ , and total cross sections for  $E_n = 0.0253$  eV and  $T = 0\text{K}$  with the corresponding ENDF/B-VI quantities, which are based principally on the compilation of Mughabghab [15]. The capture cross section values in Table III include the DC contribution. Agreement between our values and ENDF/B-VI cross sections is excellent for both  $^{35}\text{Cl}$  and  $^{37}\text{Cl}$ . The thermal  $^{35}\text{Cl}(n,p)$  cross section was discussed in section III.B.

Also given in Table III is the resonance capture integral,  $I_\gamma$ . The  $I_\gamma$  values from the present evaluation are in good agreement with the corresponding ENDF/B-VI values as would be expected from the agreement found for the thermal cross sections.

TABLE III: Cl Thermal Cross Sections and Resonance Integrals for T = 0K

Nuclide	Quantity	ENDF/B-VI (barns)	Present Evaluation (barns)
$^{35}\text{Cl}$	$\sigma_{total}$	$64.70 \pm 0.50$	64.75
	$\sigma_{elastic}$	$20.60 \pm 0.30$	20.67
	$\sigma_\gamma$	$43.60 \pm 0.40$	43.60
	$\sigma_{n,p}$	$0.48 \pm 0.14$	0.480
	$I_\gamma$	$17.80 \pm 2.00$	18.19
$^{37}\text{Cl}$	$\sigma_{total}$	$1.583 \pm 0.050$	1.581
	$\sigma_{elastic}$	$1.150 \pm 0.050$	1.148
	$\sigma_\gamma$	$0.433 \pm 0.006$	0.433
	$I_\gamma$	$0.204 \pm 0.040$	0.198
$^{nat}\text{Cl}$	$\sigma_{total}$	$49.40 \pm 0.50$	49.44
	$\sigma_{elastic}$	$15.90 \pm 0.30$	15.94
	$\sigma_\gamma$	$33.10 \pm 0.40$	33.14
	$\sigma_{n,p}$	$0.36 \pm 0.11$	0.36
	$I_\gamma$	$13.50 \pm 1.50$	13.83

The ENDF/B-VI values correspond to values quoted in the compilation of Mughabghab, et al. [15].  $\sigma_\gamma$  includes the direct capture cross section.

$^{35}\text{Cl}(^{37}\text{Cl})$  Abundance = 0.7577 (0.2423)

$$I_\gamma = \int_{0.5\text{eV}}^{20\text{MeV}} dE \sigma_\gamma / E$$

### E. Individual Resonance Discussion

The proton widths are significant fractions of the total widths for resonances at 398 and 4251 eV. It was difficult to obtain completely satisfactory fits to all the data for the 398 eV resonance. As shown in Fig. 10, the final proton width, 0.322 eV, gave SAMMY results that are, within uncertainties, consistent with the ORELA capture and transmission data, the  $^{35}\text{Cl}(n,p)$  data, and the total cross section data of Singh, et al. [6]. A small error in transmission determination could account for the difference at the peak ( $\sigma_{total} \approx 100b$ ) of the Singh data.

For the 4251 eV resonance, the proton width of 0.230 eV gives good fits to both capture and transmission data as well as a  $g\Gamma_n\Gamma_p/\Gamma$  value that is consistent with the (n,p) data.

Tables IV and V contain the resonance energies and widths from our evaluation for  $^{35}\text{Cl}$  and  $^{37}\text{Cl}$ , respectively. For resonances above 500 keV, the capture widths were set to the average capture width of the resonances observed in the capture measurements. Both  $^{35}\text{Cl}$  and  $^{37}\text{Cl}$  have ground state spin 3/2 and positive parity. Thus s waves give two spin groups:  $J^\pi = 1^+$  and  $2^+$ ; p waves give six spin groups:  $J^\pi = 0^-, 1^-, 2^-$  for channel spin 1 and  $1^-, 2^-, 3^-$  for channel spin 2. The angular distribution data are rather sparse. However, several resonances were relatively strong in both capture and transmission data, and it was possible

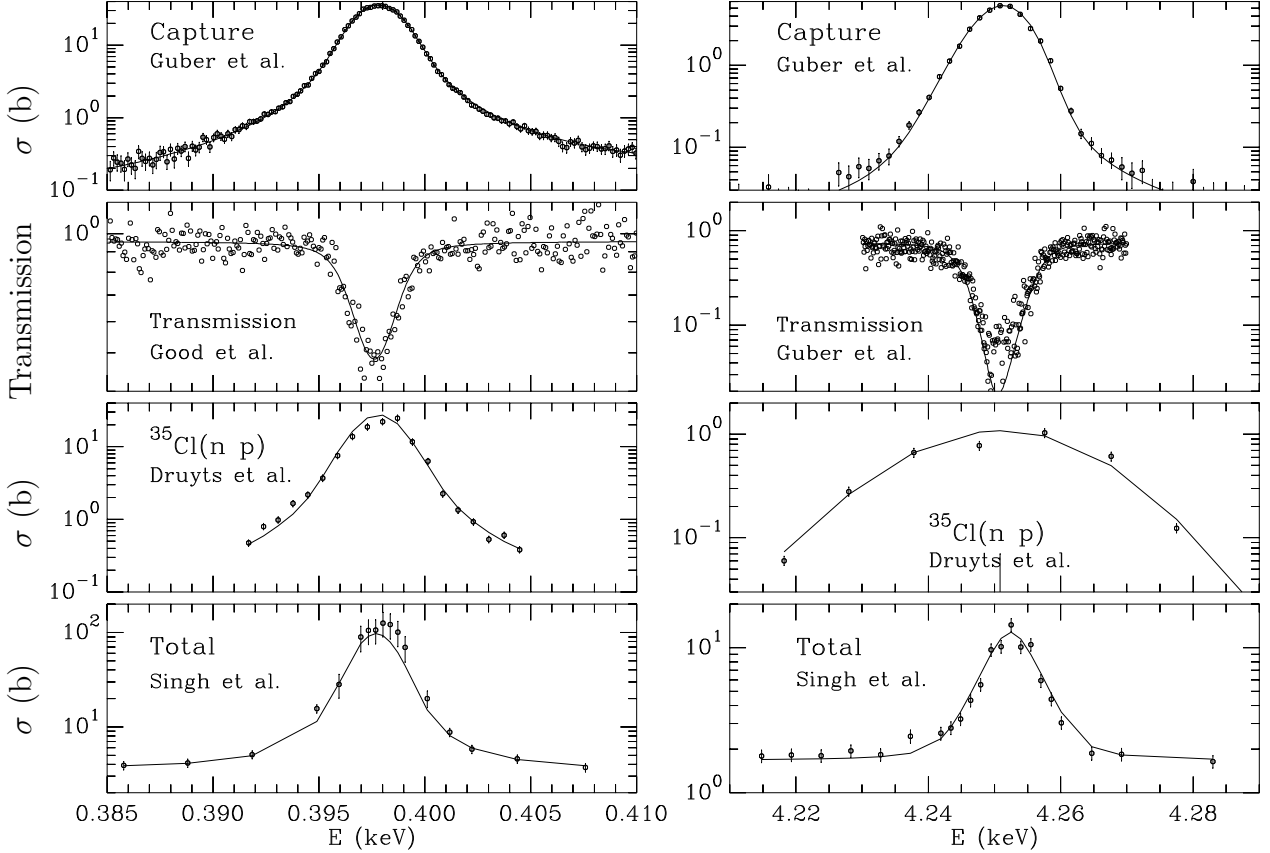


FIG. 10: Comparison of SAMMY fits (solid line) to the  $^{nat}\text{Cl}$  capture and transmission data of Guber, et al. [2], the transmission data of Good, et al. [4], the  $^{35}\text{Cl}(n,p)$  data of Druyts, et al. [12], and the total cross section data of Singh, et al. [6] for resonances at 398 and 4251 eV.

to assign these resonances to either  $^{35}\text{Cl}$  or  $^{37}\text{Cl}$  and to make unambiguous spin assignments on the basis of detailed shape and intensity analysis. In this manner, definite  $J^\pi$  values were assigned to 40 levels in  $^{35}\text{Cl}$  and 8 levels in  $^{37}\text{Cl}$ . We assumed that, for the energy region of interest ( $0 < E_n < 1.2$  MeV), d waves could be neglected. However, for 1 MeV neutrons the  $^{35}\text{Cl}$  penetrabilities for s-, p-, and d-waves are 1.030, 0.530, and 0.087, respectively. Thus, d-waves cannot be ruled out for some of the weak, higher energy resonances. Below 160 keV, the capture results reported by Macklin [23] for a sample enriched to 98.2% in  $^{37}\text{Cl}$  were utilized for the identification of several resonances belonging to  $^{37}\text{Cl}$ .

#### F. Comparison with ENDF/B-VI

In Fig. 11 we plot the  $^{35}\text{Cl}$  total cross section for  $T = 300\text{K}$  as given by the ENDF/B-VI parameters and by the present evaluation.

Between resonances, there are large differences ( $\approx 10\%$  for  $30 \text{ eV} < E_n < 2 \text{ keV}$  and  $\approx 20\%$  for  $2 \text{ keV} < E_n < 200 \text{ keV}$ ) between the two calculations. These differences reflect the more accurate recent ORELA transmission measurements. The new ORELA measurements and the older KFK measurements enabled us to extend the resonance parameter representation

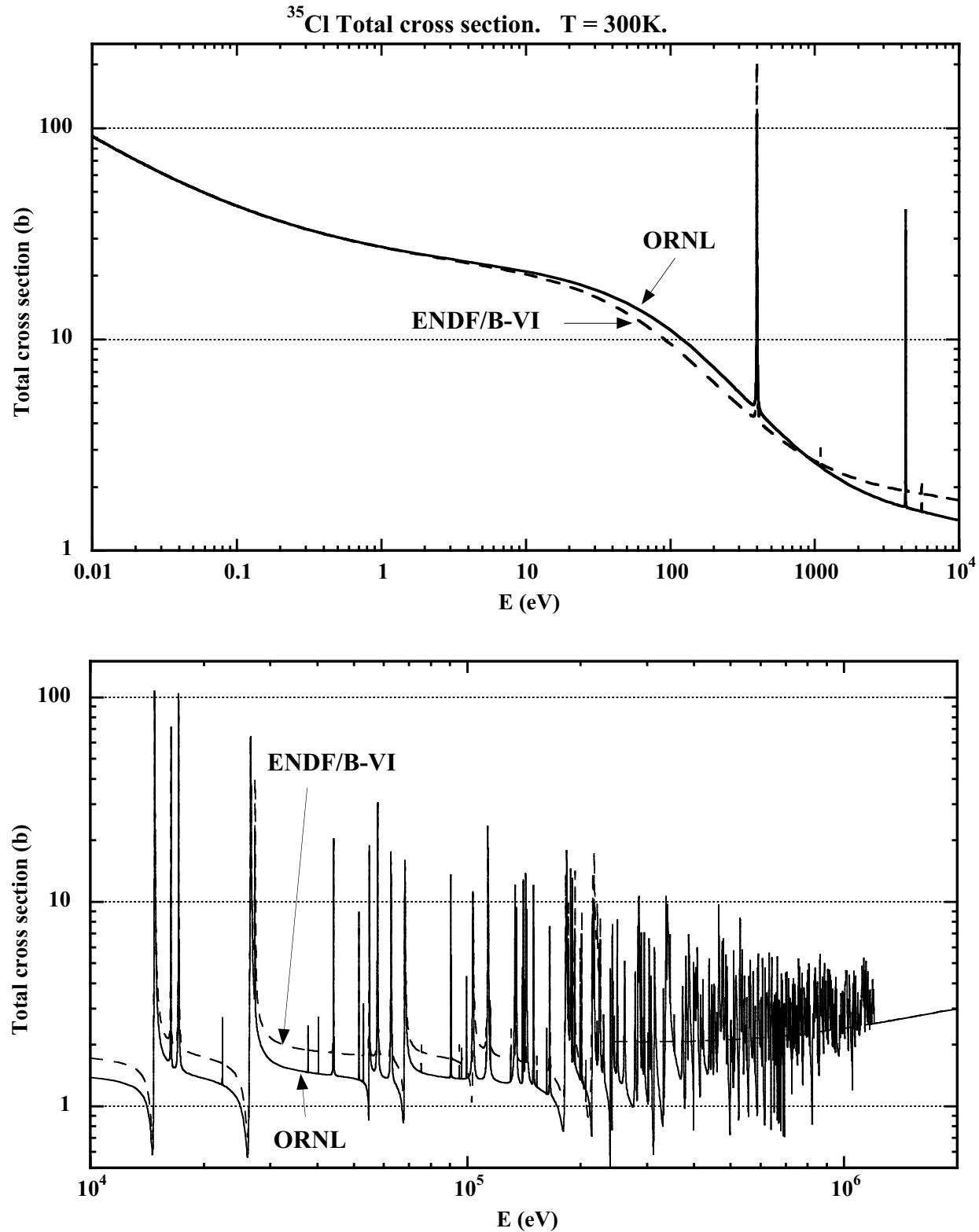


FIG. 11: Comparison of  $^{35}\text{Cl}$  total cross sections from ENDF/B-VI and the present evaluation.

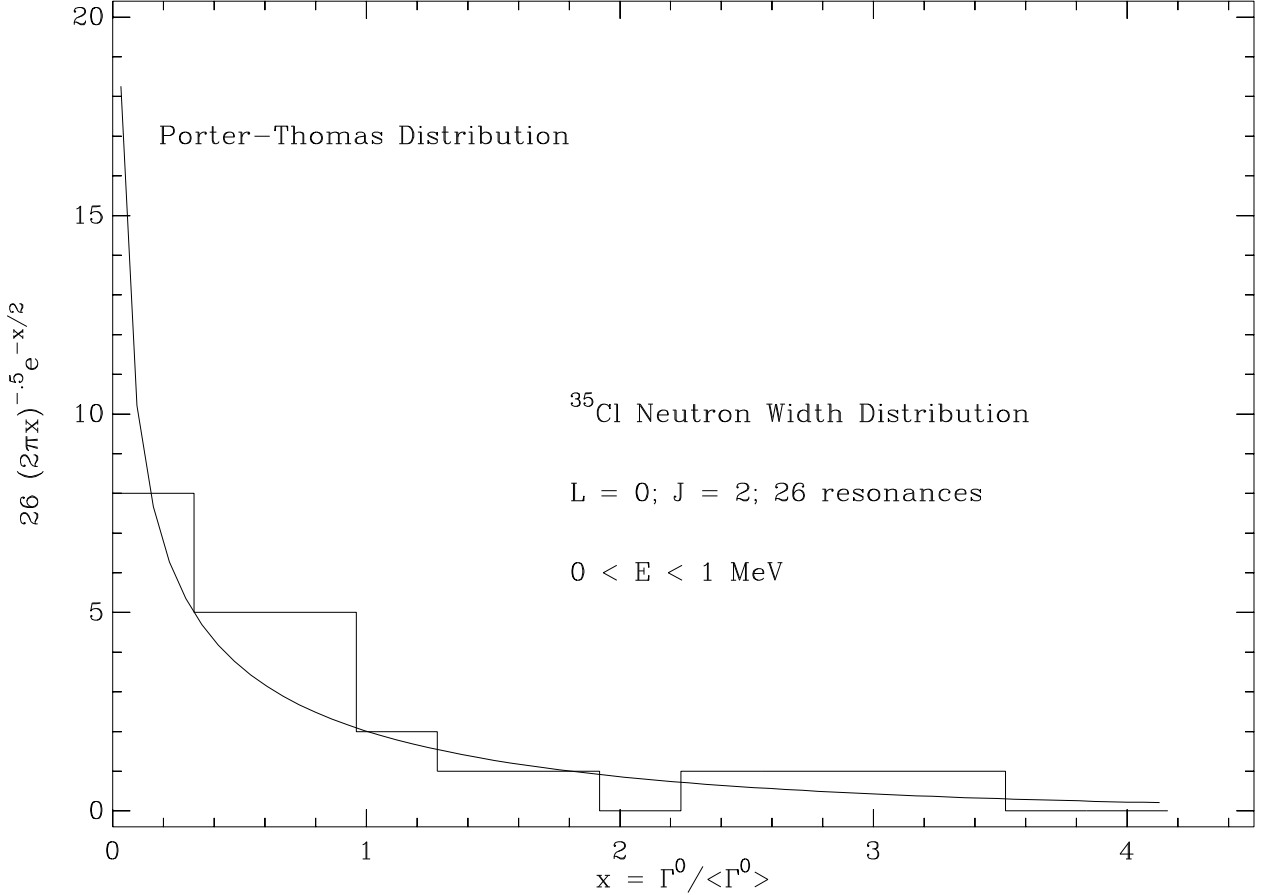


FIG. 12: Comparison of the neutron width distribution with the Porter-Thomas distribution for  $J = 2$ , s-wave  $^{35}\text{Cl}$  resonances.

to 1.2 MeV; the ENDF/B-VI representation above 226 keV, based on calculations utilizing Hauser-Feshbach statistical theory, is clearly inadequate.

### G. Level Statistics

Ideally the distribution of neutron widths corresponding to a particular spin group, e.g.  $J^\pi = 2^+$ , is expected to follow the hypothesis of Porter and Thomas [24], and the nearest neighbor level spacings are expected to be apportioned according to the Wigner distribution [25].

For our Reich-Moore representation of  $^{35}\text{Cl}$  and  $^{37}\text{Cl}$  resonance parameters, only one spin group (the  $^{35}\text{Cl} J = 2$ , s-wave group) contains a sufficient number of resonances for meaningful statistical comparisons. The distribution of  $J = 2$ , s-wave  $^{35}\text{Cl}$  neutron widths in the energy range  $0 < E_n < 1$  MeV is compared with the Porter-Thomas distribution in Fig. 12. The agreement is quite good, considering that there are only 26 resonances.

For the energy range  $0 < E_n < 1$  MeV, the distribution of  $J = 2$ , s-wave level spacings for  $^{35}\text{Cl}$  is compared with the Wigner distribution in Fig. 13. Our distribution contains more closely spaced resonances than does the Wigner distribution. However, some of these closely spaced resonances are rather weak, and the spin assignments are not definite for these weak

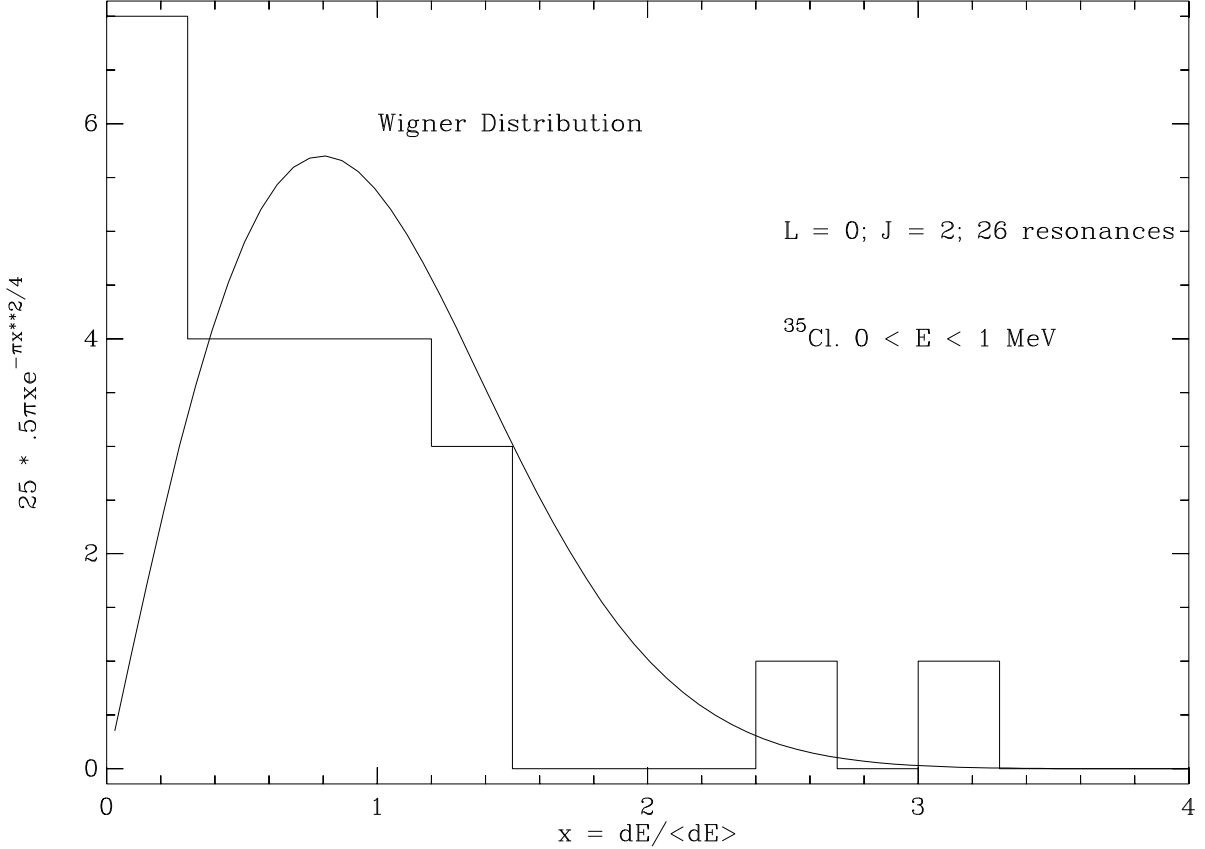


FIG. 13: Comparison of the level spacing distribution with the Wigner distribution for  $J = 2$ , s-wave  $^{35}\text{Cl}$  resonances.

resonances. We conclude that the approximate agreement with the Wigner distribution is reasonable under the circumstances.

Neutron strength function values were computed from the usual relation

$$S_l = \frac{1}{(2l+1)\Delta E} \sum g_j \Gamma_{nj}^l$$

where  $\Delta E$  is the energy interval,  $g_j$  is the statistical factor, and the reduced neutron width is given by

$$\Gamma_{nj}^l = \sqrt{\frac{1\text{eV}}{E_o}} \frac{\rho}{P_l} \Gamma_{nj}$$

$E_o$  is the resonance energy,  $P_l$  is the penetrability, and  $\rho = ka$ , where  $k$  is the wave number and  $a$  the nuclear radius. The statistical uncertainty in the strength function is  $S_l \sqrt{2/N}$ , where  $N$  is the number of resonances. Our resonance parameters yielded the following results for the range  $0 < E_n < 1$  MeV:

$^{35}\text{Cl}$ :	$10^4 S_0 = 0.59 \pm 0.12$	45 resonances
	$10^4 S_1 = 1.11 \pm 0.12$	172 resonances
$^{37}\text{Cl}$ :	$10^4 S_0 = 0.20 \pm 0.07$	19 resonances
	$10^4 S_1 = 0.65 \pm 0.09$	115 resonances

The rather small value of  $S_0$  for  $^{37}\text{Cl}$  suggests that some of the tentatively assigned p-wave resonances for  $^{37}\text{Cl}$  may, in fact, be s-wave resonances. One expects the number of resonances to be distributed roughly as  $2J + 1$ , which implies a p-wave/s-wave ratio of 3/1. For  $^{35}\text{Cl}$  the ratio is 3.8, whereas it is about 6 for  $^{37}\text{Cl}$ . The  $^{38}\text{Cl}$  structure could also play a role in reduction of the neutron strength; for example, there are only a few known positive parity levels in  $^{38}\text{Cl}$ .

#### IV. SUMMARY AND CONCLUSIONS

The Cl data used in this evaluation include recent ORELA high-resolution capture and transmission measurements as well as several older data sets. Since the  $^{35}\text{Cl}(n, p)^{35}\text{S}$  reaction yields a significant contribution to the total cross section from thermal energies up to about 10 keV, the  $^{35}\text{Cl}(n, p)$  data of Koehler [11] and Druyts, et al. [12] were fit to obtain proton width values for several resonances. The proton widths are significant fractions of the total widths for resonances at 398 and 4251 eV.

When uncertainties are considered, there is good agreement between our resonance parameter calculations and experiment for  $^{nat}\text{Cl}$  total cross sections up to  $E_n = 1200$  keV, for  $^{35}\text{Cl}(n, p)$  cross sections up to  $E_n = 100$  keV, and for  $^{nat}\text{Cl}$  capture cross sections up to 500 keV. Our thermal elastic, capture, (n,p), and total cross sections are in good agreement with the corresponding ENDF/B-VI quantities, which are based primarily on the compilation of Mughabghab [15].

The present evaluation provides resonance energies and widths for 386 s- and p-wave resonances in the range 0.2 to 1200 keV. Of these resonances, 248 are assigned to  $^{35}\text{Cl}$  and 138 to  $^{37}\text{Cl}$ .  $J^\pi$  values are assigned to 40 levels in  $^{35}\text{Cl}$  and 8 levels in  $^{37}\text{Cl}$ . Our evaluation fits the data much better than does ENDF/B-VI. This new representation should be particularly applicable to improvement of the reliability of criticality safety calculations for systems where Cl is present.

The present ENDF format does not allow for a resonance parameter representation of charged particle cross sections. A proposal is in preparation for a new ENDF format which will permit the full generality of the Reich-Moore theory, including charged particle penetrabilities.

#### V. ACKNOWLEDGMENTS

It is a pleasure to acknowledge helpful discussions with Drs. H. Derrien, J. A. Harvey, T. E. Valentine, and P. E. Koehler. We thank Dr. C. Wagemans for sending us the  $^{35}\text{Cl}(n, p)$  data of Druyts, et al.

This research was sponsored by the Office of Environmental Management, U.S. Department of Energy, under contract DE-AC05-00OR227525 with UT-Battelle, LLC.

## REFERENCES

---

- [1] P.G. Young, R.E. MacFarlane, and L.C. Liu, ENDF/B-VI MOD 1 Evaluation, February 2000.
- [2] K. H. Guber, R. O. Sayer, T. E. Valentine, L. C. Leal, R. R. Spencer, J. A. Harvey, P. E. Koehler, and T. Rauscher, *Phys. Rev.* **C65**, 058801 (2002).
- [3] N. M. Larson, ORNL/TM-9179/R5 (2000).
- [4] W. M. Good, J. A. Harvey, and N. W. Hill, ORNL-4937, p. 198 (1973); J. A. Harvey, private communication.
- [5] S. Cierjacks, P. Forti, D. Kopsch, L. Kropp, J. Nebe, and H. Unseld, "High Resolution Total Neutron Cross Sections for Na, Cl, K, V, MN and Co between 0.5 and 30 MEV", KFK-1000, (1969).
- [6] U. N. Singh, H. I. Liou, G. Hacken, M. Slagowitz, F. Rahn, J. Rainwater, W. Makofske, and J. Garg, "Neutron Resonance Spectroscopy: Chlorine", *Phys. Rev.* **C10**, 2138 (1974).
- [7] R. M. Brugger, et al., *Phys. Rev.* **104**, 1054 (1956).
- [8] R. M. Kiehn, et al., *Phys. Rev.* **91**, 66 (1953).
- [9] H. W. Newson, et al., *Phys. Rev.* **105**, 198 (1957).
- [10] N. T. Kashukeev, Yu. P. Popov, and F. L. Shapiro, *J. Nucl. Energy* **14**, 76 (1961).
- [11] P. E. Koehler, *Phys. Rev.* **C44**, 1675 (1991).
- [12] S. Druyts, C. Wagemans, and P. Geltenbort, *Nucl. Phys.* **A574**, 291 (1994).
- [13] R. O. Sayer, ORNL/TM-2000/212 (2000).
- [14] R. E. MacFarlane and D. W. Muir, LA-12740-M (1994).
- [15] S. F. Mughabghab, M. Divadeenam, N. E. Holden, Neutron Cross Sections, Vol. 1, Part A, Academic Press, Inc. (1981).
- [16] G. H. E. Sims and D. G. Juhnke, *Phys. Rev.* **165**, 1184 (1968).
- [17] I. G. Schroder, M. McKeown, and G. Scharff-Goldhaber, *J. Inorg. Nucl. Chem.* **31**, 3721 (1969).
- [18] Y. M. Gledenov, V. I. Salatski, P. V. Sedyshev, P. J. Szalanski, J. Andrzejewski, and A. Zak, Proc. Int. Conf. on Nuclear Data for Science and Technology, Trieste, p. 511 (1997).
- [19] Y. M. Gledenov, L. B. Mitsina, M. Mitukov, Y. P. Popov, J. Rigol, V. I. Salatski, and F. Van Zuan, Joint Institute for Nuclear Research, Communications **P3-89-351**, Dubna, USSR (1989).
- [20] P. E. Koehler, et al., *Phys. Rev.* **C54**, 1463 (1996).
- [21] H. Krauss, K. Grün, T. Rauscher, and H. Oberhummer, 1992, TU Wien (Vienna, Austria), code TEDCA (unpublished).
- [22] T. Rauscher, R. Bieber, H. Oberhummer, K.-L. Kratz, J. Dobaczewski, P. Möller, and M. M. Sharma, *Phys. Rev.* **C57**, 2031 (1998).
- [23] R. L. Macklin, *Phys. Rev.* **C29**, 1996 (1984).
- [24] C. E. Porter and R. G. Thomas, *Phys. Rev.* **104**, 483 (1956).
- [25] E. P. Wigner, Can. Math. Congr. Proc., Toronto, p 174 (1957); *Ann. Math.* **67**, 325 (1958).

TABLE IV: Energies and Widths for Resonances in  $^{35}\text{Cl}$  (n,X)

Res. Num.	$E_R$ (keV)	$J^\pi$	$\Gamma_\gamma$ (meV)	$\Gamma_n$ (eV)	$\Gamma_p$ (eV)
1	-336.93	(2 <sup>-</sup> )	534.	38202.	
2	-0.18065	(2 <sup>+</sup> )	530.	13.28	0.00599
3	0.39782	2 <sup>-</sup>	665.	0.05050	0.3220
4	4.2508	1 <sup>-</sup>	472.	0.6280	0.2300
5	5.4910	(1 <sup>-</sup> )	970.	0.00386	
6	14.802	2 <sup>+</sup>	346.	32.60	0.0280
7	16.356	(3 <sup>-</sup> )	386.	5.982	0.1640
8	17.134	3 <sup>-</sup>	802.	14.10	0.0320
9	22.396	(0 <sup>-</sup> )	1725.	0.9664	
10	26.616	2 <sup>+</sup>	304.	115.5	
11	27.346	(2 <sup>-</sup> )	458.	6.028	0.1470
12	37.768	(1 <sup>-</sup> )	191.	0.4408	
13	40.270	(3 <sup>-</sup> )	577.	0.1773	
14	44.166	(1 <sup>-</sup> )	1043.	30.55	
15	51.608	(3 <sup>-</sup> )	45.	2.417	0.0960
16	52.974	(2 <sup>-</sup> )	562.	0.8159	
17	54.932	1 <sup>+</sup>	367.	46.44	
18	57.812	(2 <sup>-</sup> )	538.	107.4	0.9980
19	62.779	1 <sup>-</sup>	621.	134.6	
20	68.236	1 <sup>+</sup>	393.	217.9	
21	75.495	(3 <sup>-</sup> )	806.	0.07992	
22	90.420	(2 <sup>-</sup> )	716.	21.79	0.2740
23	90.526	(2 <sup>-</sup> )	128.	4.235	
24	95.207	(3 <sup>-</sup> )	453.	0.1549	
25	96.604	(0 <sup>-</sup> )	1565.	2.761	
26	99.441	(3 <sup>-</sup> )	232.	2.393	
27	103.52	1 <sup>-</sup>	388.	382.0	1.973
28	112.05	(3 <sup>-</sup> )	324.	0.2642	
29	113.40	(2 <sup>-</sup> )	337.	142.3	
30	113.61	(2 <sup>-</sup> )	295.	397.2	
31	115.12	(1 <sup>-</sup> )	767.	4.308	
32	130.44	(2 <sup>-</sup> )	759.	0.7666	
33	133.99	(1 <sup>-</sup> )	2314.	660.1	
34	135.12	1 <sup>-</sup>	341.	187.5	
35	140.09	(3 <sup>-</sup> )	366.	3.778	
36	140.83	(2 <sup>-</sup> )	546.	98.71	
37	141.64	(3 <sup>-</sup> )	313.	3.954	
38	143.02	(2 <sup>-</sup> )	492.	314.7	
39	149.83	(2 <sup>-</sup> )	756.	113.2	
40	152.92	(3 <sup>-</sup> )	299.	0.3821	
41	162.56	(1 <sup>-</sup> )	647.	5.635	

TABLE IV: Energies and Widths for Resonances in  $^{35}\text{Cl}$  (n,X), cont.

Res. Num.	$E_R$ (keV)	$J^\pi$	$\Gamma_\gamma$ (meV)	$\Gamma_n$ (eV)	$\Gamma_p$ (eV)
42	165.48	(1 <sup>-</sup> )	1050.	207.3	
43	182.52	1 <sup>+</sup>	745.	1760.	
44	183.54	(3 <sup>-</sup> )	333.	461.5	
45	185.28	(3 <sup>-</sup> )	466.		4.482
46	188.15	3 <sup>-</sup>	498.	422.2	
47	190.18	(3 <sup>-</sup> )	294.	102.5	
48	192.94	(3 <sup>-</sup> )	756.		16.36
49	192.68	(2 <sup>-</sup> )	229.		33.81
50	199.17	(3 <sup>-</sup> )	255.		2.776
51	201.09	(2 <sup>-</sup> )	291.		36.50
52	205.97	(2 <sup>-</sup> )	451.		0.5888
53	206.62	(2 <sup>-</sup> )	594.		0.5594
54	214.55	(2 <sup>-</sup> )	232.		42.38
55	214.92	2 <sup>+</sup>	349.		652.8
56	215.35	(2 <sup>-</sup> )	774.		4.559
57	217.10	2 <sup>-</sup>	619.		577.2
58	219.99	(1 <sup>-</sup> )	400.		3.848
59	221.39	(2 <sup>-</sup> )	1593.		4.073
60	224.11	1 <sup>-</sup>	403.		756.7
61	225.14	1 <sup>-</sup>	1346.		568.5
62	228.89	(1 <sup>-</sup> )	594.		1.769
63	230.07	(0 <sup>-</sup> )	324.		811.8
64	239.74	(1 <sup>+</sup> )	687.		268.5
65	242.60	(2 <sup>+</sup> )	902.		344.0
66	243.22	(0 <sup>-</sup> )	703.		217.4
67	245.48	(0 <sup>-</sup> )	832.		6.556
68	245.85	(2 <sup>-</sup> )	765.		5.612
69	250.20	2 <sup>-</sup>	405.		434.6
70	261.55	1 <sup>-</sup>	846.		1064.
71	279.11	1 <sup>-</sup>	377.		1254.
72	283.75	(2 <sup>-</sup> )	647.		423.7
73	284.50	(1 <sup>-</sup> )	905.		4.162
74	284.66	(2 <sup>+</sup> )	499.		1194.
75	285.61	(2 <sup>-</sup> )	842.		1569.
76	287.01	(2 <sup>-</sup> )	554.		21.26
77	290.08	(2 <sup>-</sup> )	1615.		152.1
78	293.38	(3 <sup>-</sup> )	1803.		5.942
79	294.95	(2 <sup>-</sup> )	739.		474.7
80	301.45	(2 <sup>-</sup> )	402.		8.856
81	303.84	2 <sup>-</sup>	1698.		695.7
82	306.03	1 <sup>-</sup>	563.		7.718

TABLE IV: Energies and Widths for Resonances in  $^{35}\text{Cl}$  (n,X), cont.

Res. Num.	$E_R$ (keV)	$J^\pi$	$\Gamma_\gamma$ (meV)	$\Gamma_n$ (eV)	$\Gamma_p$ (eV)
83	307.41	(1 <sup>-</sup> )	640.	1172.	
84	313.75	2 <sup>+</sup>	476.	1476.	
85	331.22	(2 <sup>-</sup> )	398.	33.23	
86	335.13	(1 <sup>+</sup> )	358.	5526.	
87	336.76	(3 <sup>-</sup> )	416.	289.0	
88	338.98	(2 <sup>+</sup> )	2383.	877.8	
89	340.70	1 <sup>-</sup>	565.	3875.	
90	341.34	(0 <sup>-</sup> )	655.	5720.	
91	345.55	(2 <sup>-</sup> )	348.	63.19	
92	354.38	(2 <sup>-</sup> )	233.	8.058	
93	372.90	1 <sup>-</sup>	2108.	1796.	
94	380.26	(2 <sup>+</sup> )	463.	1179.	
95	381.97	(1 <sup>-</sup> )	8184.	1.603	
96	384.47	(2 <sup>-</sup> )	5786.	1.986	
97	386.42	(2 <sup>+</sup> )	418.	1240.	
98	387.89	(1 <sup>-</sup> )	911.	3239.	
99	399.15	(1 <sup>+</sup> )	741.	1094.	
100	401.92	1 <sup>-</sup>	333.	1212.	
101	404.47	1 <sup>-</sup>	1492.	1010.	
102	407.82	2 <sup>-</sup>	551.	2040.	
103	415.67	(1 <sup>+</sup> )	329.	1146.	
104	422.10	(1 <sup>-</sup> )	2868.	857.7	
105	438.65	(2 <sup>-</sup> )	645.	1274.	
106	444.48	(2 <sup>-</sup> )	205.	181.0	
107	450.63	(1 <sup>+</sup> )	393.	461.3	
108	451.38	(2 <sup>-</sup> )	1760.	5.759	
109	452.63	(1 <sup>-</sup> )	860.	3431.	
110	457.89	(2 <sup>-</sup> )	1147.	7.323	
111	459.41	(1 <sup>-</sup> )	616.	42.64	
112	465.34	(1 <sup>-</sup> )	367.	693.9	
113	465.50	2 <sup>-</sup>	558.	4040.	
114	469.10	(2 <sup>-</sup> )	952.	3.761	
115	475.30	3 <sup>-</sup>	830.	2792.	
116	477.20	(2 <sup>-</sup> )	540.	165.9	
117	481.28	(0 <sup>-</sup> )	782.	1774.	
118	483.69	(1 <sup>-</sup> )	1907.	2735.	
119	485.46	(2 <sup>-</sup> )	1273.	480.0	
120	488.63	(2 <sup>+</sup> )	408.	780.7	
121	499.79	(1 <sup>+</sup> )	670.	2312.	
122	504.86	(0 <sup>-</sup> )	839.	679.1	
123	509.76	(3 <sup>-</sup> )	839.	387.0	

TABLE IV: Energies and Widths for Resonances in  $^{35}\text{Cl}$  (n,X), cont.

Res. Num.	$E_R$ (keV)	$J^\pi$	$\Gamma_\gamma$ (meV)	$\Gamma_n$ (eV)	$\Gamma_p$ (eV)
124	514.40	$2^+$	561.	5284.	
125	527.94	$(2^+)$	561.	2812.	
126	529.90	$(3^-)$	839.	1354.	
127	535.25	$(3^-)$	839.	448.1	
128	542.22	$(1^+)$	561.	522.0	
129	543.78	$(2^-)$	839.	691.7	
130	547.85	$(0^-)$	839.	764.0	
131	552.63	$(1^-)$	839.	279.1	
132	559.03	$(2^+)$	561.	1813.	
133	559.25	$(1^-)$	839.	585.7	
134	564.58	$(2^-)$	839.	536.0	
135	573.88	$(2^-)$	839.	1470.	
136	581.18	$(1^-)$	839.	208.8	
137	590.81	$(2^+)$	561.	3236.	
138	590.36	$(2^-)$	839.	755.0	
139	591.34	$(1^-)$	839.	167.4	
140	600.84	$(1^-)$	839.	1209.	
141	608.06	$(3^-)$	839.	774.8	
142	614.26	$(1^-)$	499.	1153.	
143	618.10	$(2^-)$	839.	1075.	
144	621.68	$(2^+)$	561.	6759.	
145	629.58	$(1^-)$	839.	622.5	
146	631.04	$2^+$	561.	1637.	
147	633.10	$(2^-)$	839.	144.5	
148	640.81	$2^+$	561.	859.7	
149	642.74	$(2^-)$	839.	949.9	
150	649.26	$(1^+)$	561.	568.3	
151	653.69	$(2^+)$	561.	372.7	
152	658.15	$(1^+)$	561.	273.3	
153	659.32	$(1^-)$	839.	104.8	
154	664.93	$(2^+)$	561.	96.12	
155	665.71	$(3^-)$	839.	250.8	
156	669.96	$(1^+)$	561.	316.3	
157	672.16	$(2^+)$	561.	349.9	
158	673.98	$(3^-)$	561.	48.96	
159	678.00	$(1^+)$	561.	133.2	
160	681.06	$(2^+)$	561.	665.5	
161	681.67	$(3^-)$	839.	60.29	
162	685.02	$(3^-)$	839.	117.3	
163	690.58	$(2^+)$	561.	591.5	
164	694.63	$(2^+)$	561.	864.5	

TABLE IV: Energies and Widths for Resonances in  $^{35}\text{Cl}$  (n,X), cont.

Res. Num.	$E_R$ (keV)	$J^\pi$	$\Gamma_\gamma$ (meV)	$\Gamma_n$ (eV)	$\Gamma_p$ (eV)
165	701.00	(3 $^-$ )	839.	1252.	
166	703.62	(2 $^-$ )	839.	931.1	
167	712.53	2 $^-$	839.	3301.	
168	718.38	(1 $^-$ )	839.	974.0	
169	721.99	(1 $^-$ )	839.	826.8	
170	725.18	(1 $^+$ )	561.	167.2	
171	729.58	(2 $^-$ )	839.	646.6	
172	732.89	(1 $^-$ )	839.	1956.	
173	735.01	(2 $^-$ )	839.	377.8	
174	739.81	2 $^-$	839.	3042.	
175	748.48	(1 $^-$ )	839.	1024.	
176	754.69	(1 $^+$ )	561.	2691.	
177	757.46	3 $^-$	839.	3780.	
178	761.11	3 $^-$	839.	2239.	
179	765.41	(1 $^-$ )	839.	1520.	
180	770.29	(2 $^-$ )	839.	3185.	
181	774.97	(3 $^-$ )	839.	368.9	
182	779.97	(2 $^+$ )	561.	5311.	
183	781.46	(1 $^+$ )	561.	1294.	
184	792.67	(1 $^-$ )	839.	1216.	
185	798.56	(2 $^-$ )	839.	2911.	
186	801.33	(2 $^-$ )	839.	680.7	
187	806.88	(3 $^-$ )	839.	629.8	
188	810.34	(1 $^-$ )	839.	508.9	
189	824.95	(2 $^+$ )	561.	2764.	
190	827.38	(2 $^-$ )	561.	436.1	
191	831.58	(1 $^+$ )	839.	445.3	
192	832.26	(2 $^-$ )	839.	1383.	
193	835.85	(2 $^-$ )	839.	1181.	
194	838.95	(3 $^-$ )	839.	3395.	
195	845.15	(1 $^-$ )	839.	4177.	
196	848.41	(2 $^-$ )	839.	2391.	
197	852.49	(2 $^-$ )	839.	1727.	
198	860.96	2 $^+$	561.	7202.	
199	862.61	(3 $^-$ )	839.	694.6	
200	871.57	(1 $^-$ )	839.	1987.	
201	876.99	(2 $^-$ )	839.	575.7	
202	882.98	(1 $^+$ )	561.	978.1	
203	886.58	3 $^-$	839.	3198.	
204	895.07	(2 $^-$ )	839.	1506.	
205	905.86	(3 $^-$ )	839.	441.2	

TABLE IV: Energies and Widths for Resonances in  $^{35}\text{Cl}$  (n,X), cont.

Res. Num.	$E_R$ (keV)	$J^\pi$	$\Gamma_\gamma$ (meV)	$\Gamma_n$ (eV)	$\Gamma_p$ (eV)
206	910.90	(3 $^-$ )	839.	3339.	
207	915.65	(2 $^-$ )	839.	1034.	
208	922.52	(2 $^-$ )	839.	1572.	
209	933.14	(2 $^-$ )	839.	938.7	
210	936.66	(1 $^-$ )	839.	606.1	
211	943.95	(1 $^-$ )	839.	555.6	
212	946.10	(2 $^-$ )	839.	480.6	
213	950.47	(3 $^-$ )	839.	645.1	
214	953.35	(2 $^-$ )	839.	1001.	
215	974.75	(1 $^-$ )	839.	3259.	
216	981.04	(2 $^-$ )	839.	4229.	
217	984.51	(1 $^-$ )	839.	1802.	
218	991.54	(2 $^-$ )	839.	4348.	
219	999.85	(2 $^-$ )	839.	3022.	
220	1006.5	(2 $^-$ )	839.	3591.	
221	1010.4	(3 $^-$ )	839.	7910.	
222	1016.5	(2 $^-$ )	839.	4020.	
223	1028.5	(2 $^-$ )	839.	2389.	
224	1033.7	3 $^-$	839.	3550.	
225	1050.6	(2 $^-$ )	839.	1304.	
226	1053.4	2 $^+$	561.	2038.	
227	1055.5	(2 $^-$ )	839.	3889.	
228	1062.1	(3 $^-$ )	839.	420.8	
229	1071.2	(3 $^-$ )	839.	1944.	
230	1074.0	(2 $^-$ )	839.	1039.	
231	1080.2	(2 $^-$ )	839.	751.2	
232	1085.4	(3 $^-$ )	839.	134.0	
233	1088.7	(2 $^-$ )	839.	5239.	
234	1092.0	(1 $^-$ )	839.	1975.	
235	1103.7	(3 $^-$ )	839.	1609.	
236	1109.2	(1 $^+$ )	561.	2742.	
237	1115.7	(2 $^-$ )	839.	3444.	
238	1116.0	(2 $^-$ )	839.	43637.	
239	1120.9	(3 $^-$ )	499.	389.0	
240	1126.9	(3 $^-$ )	839.	615.5	
241	1132.0	(2 $^-$ )	839.	1523.	
242	1137.9	(2 $^+$ )	561.	1836.	
243	1138.7	(1 $^-$ )	839.	954.4	
244	1144.9	(3 $^-$ )	839.	1587.	
245	1155.3	(3 $^-$ )	839.	1578.	
246	1165.3	(2 $^-$ )	839.	7310.	

TABLE IV: Energies and Widths for Resonances in  $^{35}\text{Cl}$  (n,X), cont.

Res. Num.	$E_R$ (keV)	$J^\pi$	$\Gamma_\gamma$ (meV)	$\Gamma_n$ (eV)	$\Gamma_p$ (eV)
247	1172.1	(2 <sup>-</sup> )	839.	1495.	
248	1177.0	(1 <sup>-</sup> )	839.	1488.	
249	1189.7	(3 <sup>-</sup> )	839.	7290.	
250	1198.5	(2 <sup>-</sup> )	839.	3243.	
251	1205.7	(1 <sup>+</sup> )	561.	642.6	
252	1209.0	(3 <sup>-</sup> )	839.	3485.	
253	1218.1	(2 <sup>-</sup> )	839.	3247.	
254	1225.3	(1 <sup>-</sup> )	839.	1807.	
255	1237.2	(3 <sup>-</sup> )	839.	5888.	
256	1243.5	(2 <sup>-</sup> )	839.	3097.	
257	1257.7	(2 <sup>+</sup> )	561.	1750.	
258	1268.6	(3 <sup>-</sup> )	839.	2391.	
259	1277.7	(3 <sup>-</sup> )	839.	2984.	
260	1283.8	(2 <sup>-</sup> )	839.	5041.	
261	1311.8	(2 <sup>-</sup> )	839.	794.6	
262	1315.1	(3 <sup>-</sup> )	839.	12106.	
263	1337.1	(2 <sup>-</sup> )	839.	4850.	
264	1353.6	(1 <sup>-</sup> )	839.	38797.	
265	1354.1	(2 <sup>-</sup> )	839.	11033.	
266	1366.1	(2 <sup>-</sup> )	839.	8350.	
267	1390.7	(3 <sup>-</sup> )	839.	5502.	
268	1403.9	(2 <sup>-</sup> )	839.	8067.	
269	1425.4	(3 <sup>-</sup> )	839.	13820.	
270	1434.3	(2 <sup>-</sup> )	839.	5423.	
271	1435.5	(1 <sup>-</sup> )	839.	5366.	
272	1441.4	(2 <sup>-</sup> )	839.	1609.	
273	1485.1	(3 <sup>-</sup> )	839.	10541.	
274	7563.1	(2 <sup>+</sup> )	384.	621905.	

Capture widths for  $500 < E_n < 1500$  keV were set to average capture widths for  $0 < E_n < 500$  keV: 561 meV for s-waves and 839 meV for p-waves.

Positive parity levels are s-waves; negative parity levels are p-waves.

The  $^{35}\text{Cl}$  nuclear radius used to compute penetrabilities and shifts was 4.8222 fm. Radii for potential scattering were  $R(l=0,1) = 3.6680, 4.8888$  fm.

Tentative spin-parity assignments are indicated by parentheses.

TABLE V: Energies and Widths for Resonances in  $^{37}\text{Cl}$  (n,X)

Res. Num.	$E_R$ (keV)	$J^\pi$	$\Gamma_\gamma$ (meV)	$\Gamma_n$ (eV)
1	-1.0000	(1 <sup>+</sup> )	225	9.556
2	8.3208	2 <sup>+</sup>	196.	78.70
3	25.579	1 <sup>+</sup>	513.	652.2
4	27.824	(2 <sup>-</sup> )	79.	5.537
5	32.187	(1 <sup>-</sup> )	82.	10.53
6	42.358	(1 <sup>-</sup> )	260.	0.2789
7	46.653	2 <sup>+</sup>	265.	390.5
8	51.548	(3 <sup>-</sup> )	78.	3.329
9	55.146	(0 <sup>-</sup> )	70.	3.921
10	55.440	2 <sup>-</sup>	179.	122.8
11	66.707	(2 <sup>-</sup> )	107.	25.92
12	66.837	(2 <sup>-</sup> )	154.	50.88
13	86.211	(1 <sup>-</sup> )	252.	1.103
14	93.138	2 <sup>+</sup>	221.	726.6
15	97.903	(0 <sup>-</sup> )	1882.	2.691
16	114.74	(0 <sup>-</sup> )	331.	250.0
17	125.26	(3 <sup>-</sup> )	6.	31.11
18	125.51	(3 <sup>-</sup> )	6.	26.38
19	127.76	(2 <sup>+</sup> )	268.	391.0
20	128.22	(1 <sup>-</sup> )	281.	35.49
21	135.43	(0 <sup>-</sup> )	238.	163.9
22	136.28	2 <sup>+</sup>	262.	1392.
23	143.72	(3 <sup>-</sup> )	171.	653.0
24	144.34	(1 <sup>-</sup> )	154.	64.09
25	150.08	(1 <sup>-</sup> )	515.	89.65
26	150.67	(2 <sup>-</sup> )	412.	12.66
27	157.56	(2 <sup>-</sup> )	166.	148.9
28	164.95	(0 <sup>-</sup> )	1176.	214.9
29	166.47	(1 <sup>-</sup> )	827.	86.59
30	167.30	(1 <sup>-</sup> )	286.	51.55
31	168.96	(2 <sup>-</sup> )	151.	248.0
32	176.72	(2 <sup>-</sup> )	361.	166.2
33	177.61	(0 <sup>-</sup> )	488.	458.5
34	179.86	(1 <sup>+</sup> )	216.	1610.
35	179.91	(1 <sup>-</sup> )	216.	116.8
36	187.00	(2 <sup>+</sup> )	318.	308.5
37	190.70	(1 <sup>+</sup> )	464.	1111.
38	191.13	(1 <sup>-</sup> )	392.	184.4
39	208.35	(1 <sup>+</sup> )	115.	519.4
40	213.23	(1 <sup>-</sup> )	1277.	25.91
41	214.16	(0 <sup>-</sup> )	1718.	271.2

TABLE V: Energies and Widths for Resonances in  $^{37}\text{Cl}$  (n,X), cont.

Res. Num.	$E_R$ (keV)	$J^\pi$	$\Gamma_\gamma$ (meV)	$\Gamma_n$ (eV)
42	217.68	(0 <sup>-</sup> )	3104.	430.7
43	218.66	(0 <sup>-</sup> )	358.	151.0
44	219.68	(0 <sup>-</sup> )	356.	107.2
45	221.15	(2 <sup>+</sup> )	201.	65.16
46	226.69	(2 <sup>-</sup> )	447.	4.301
47	227.66	(0 <sup>-</sup> )	919.	44.28
48	229.90	(0 <sup>-</sup> )	241.	248.8
49	244.09	(3 <sup>-</sup> )	235.	22.95
50	248.45	(2 <sup>+</sup> )	267.	133.1
51	254.03	2 <sup>-</sup>	366.	694.0
52	254.78	(1 <sup>-</sup> )	548.	63.99
53	255.66	(1 <sup>-</sup> )	876.	60.45
54	256.84	(2 <sup>-</sup> )	1514.	45.06
55	259.25	(2 <sup>-</sup> )	1636.	43.27
56	262.44	(2 <sup>-</sup> )	577.	73.10
57	263.86	(0 <sup>-</sup> )	365.	186.4
58	265.84	(1 <sup>-</sup> )	917.	65.70
59	278.12	(0 <sup>-</sup> )	362.	109.0
60	280.60	(2 <sup>-</sup> )	302.	71.44
61	281.67	(1 <sup>-</sup> )	318.	131.8
62	288.35	(3 <sup>-</sup> )	359.	36.77
63	298.77	(3 <sup>-</sup> )	818.	13.57
64	301.17	(1 <sup>-</sup> )	376.	400.7
65	308.95	(1 <sup>-</sup> )	332.	515.3
66	311.06	(2 <sup>-</sup> )	349.	2369.
67	316.69	(0 <sup>-</sup> )	369.	223.1
68	333.38	(3 <sup>-</sup> )	365.	169.1
69	334.53	(1 <sup>-</sup> )	366.	1158.
70	336.00	(1 <sup>-</sup> )	358.	789.5
71	358.38	(2 <sup>+</sup> )	218.	764.2
72	360.74	(2 <sup>-</sup> )	338.	196.8
73	368.40	(2 <sup>-</sup> )	332.	98.21
74	377.17	(0 <sup>-</sup> )	945.	3368.
75	379.39	(3 <sup>-</sup> )	383.	869.5
76	383.65	(2 <sup>-</sup> )	841.	2132.
77	391.89	(2 <sup>-</sup> )	383.	84.09
78	394.49	(0 <sup>-</sup> )	384.	80.11
79	411.72	(2 <sup>-</sup> )	361.	213.5
80	414.24	(1 <sup>-</sup> )	352.	3035.
81	415.19	(2 <sup>-</sup> )	336.	921.3
82	417.05	(2 <sup>-</sup> )	349.	228.6

TABLE V: Energies and Widths for Resonances in  $^{37}\text{Cl}$  (n,X), cont.

Res. Num.	$E_R$ (keV)	$J^\pi$	$\Gamma_\gamma$ (meV)	$\Gamma_n$ (eV)
83	417.86	(2 <sup>-</sup> )	351.	3150.
84	424.04	(3 <sup>-</sup> )	374.	328.0
85	425.18	(2 <sup>-</sup> )	347.	602.8
86	427.53	(3 <sup>-</sup> )	1056.	150.4
87	431.03	(2 <sup>+</sup> )	258.	144.1
88	434.21	(2 <sup>+</sup> )	356.	95.03
89	435.89	(2 <sup>-</sup> )	396.	153.3
90	446.39	3 <sup>-</sup>	470.	2215.
91	491.52	(1 <sup>-</sup> )	325.	3532.
92	495.58	(2 <sup>-</sup> )	325.	893.7
93	498.17	(2 <sup>-</sup> )	1440.	2393.
94	500.36	(2 <sup>-</sup> )	404.	1754.
95	507.97	(1 <sup>+</sup> )	270.	3127.
96	513.60	(1 <sup>-</sup> )	499.	197.0
97	516.62	(2 <sup>-</sup> )	499.	1078.
98	523.39	(1 <sup>-</sup> )	499.	939.1
99	525.73	(3 <sup>-</sup> )	499.	858.0
100	553.89	(1 <sup>-</sup> )	499.	1967.
101	557.17	(2 <sup>-</sup> )	499.	793.8
102	569.51	(1 <sup>-</sup> )	499.	476.7
103	571.44	(0 <sup>-</sup> )	499.	1072.
104	576.36	(2 <sup>-</sup> )	499.	1108.
105	578.39	(1 <sup>-</sup> )	499.	1372.
106	584.89	(1 <sup>-</sup> )	499.	697.0
107	586.87	(0 <sup>-</sup> )	499.	843.8
108	588.40	(3 <sup>-</sup> )	499.	643.8
109	596.99	(1 <sup>-</sup> )	499.	574.5
110	603.98	(1 <sup>-</sup> )	499.	1054.
111	606.03	(0 <sup>-</sup> )	499.	1029.
112	610.42	(2 <sup>-</sup> )	499.	1386.
113	611.86	(1 <sup>-</sup> )	499.	990.4
114	627.24	(2 <sup>+</sup> )	270.	911.9
115	634.68	(2 <sup>-</sup> )	499.	921.5
116	636.77	(3 <sup>-</sup> )	499.	832.6
117	651.62	(2 <sup>-</sup> )	499.	1013.
118	693.38	(2 <sup>-</sup> )	499.	230.7
119	708.42	(3 <sup>-</sup> )	499.	1044.
120	742.45	(2 <sup>-</sup> )	499.	465.3
121	747.62	(2 <sup>+</sup> )	270.	299.2
122	820.59	(3 <sup>-</sup> )	499.	3126.
123	865.90	(2 <sup>-</sup> )	499.	6575.

TABLE V: Energies and Widths for Resonances in  $^{37}\text{Cl}$  (n,X), cont.

Res. Num.	$E_R$ (keV)	$J^\pi$	$\Gamma_\gamma$ (meV)	$\Gamma_n$ (eV)
124	890.16	(2 <sup>-</sup> )	499.	1235.
125	899.99	(2 <sup>-</sup> )	499.	570.9
126	919.00	(1 <sup>-</sup> )	499.	997.4
127	925.24	(3 <sup>-</sup> )	499.	401.8
128	926.96	(2 <sup>-</sup> )	499.	1458.
129	942.19	(1 <sup>-</sup> )	499.	940.4
130	958.82	(2 <sup>-</sup> )	499.	1138.
131	962.41	(3 <sup>-</sup> )	499.	1255.
132	967.39	(2 <sup>-</sup> )	499.	1209.
133	970.67	(3 <sup>-</sup> )	499.	1805.
134	995.44	(2 <sup>-</sup> )	499.	2934.
135	1024.2	(2 <sup>-</sup> )	499.	2600.
136	1038.0	(2 <sup>-</sup> )	499.	2262.
137	1044.1	(2 <sup>-</sup> )	499.	1683.
138	1083.3	(2 <sup>+</sup> )	499.	1641.
139	1098.5	(2 <sup>-</sup> )	499.	1527.
140	1214.9	(2 <sup>-</sup> )	499.	4254.
141	1292.7	(2 <sup>-</sup> )	499.	4327.
142	1304.4	(3 <sup>-</sup> )	499.	12935.
143	1386.8	(3 <sup>-</sup> )	499.	29158.
144	1482.1	(2 <sup>+</sup> )	270.	7118.
145	1809.6	(1 <sup>+</sup> )	384.	303262.

Capture widths for  $500 < E_n < 1500$  keV were set to average capture widths for  $0 < E_n < 500$  keV:  
 270 meV for s-waves and 499 meV for p-waves.

Positive parity levels are s-waves; negative parity levels are p-waves.

The  $^{37}\text{Cl}$  radius used for penetrabilities and shifts was 4.8974 fm.  
 Radii for potential scattering were  $R(l=0,1) = 3.3651, 3.9565$  fm.

Tentative spin-parity assignments are indicated by parentheses.

## INTERNAL DISTRIBUTION

- |                     |                               |
|---------------------|-------------------------------|
| 1. B. L. Broadhead  | 14. P. E. Koehler             |
| 2. H. Derrien       | 15. N. M. Larson              |
| 3. M. E. Dunn       | 16. L. C. Leal                |
| 4. C. Y. Fu         | 17. C. V. Parks               |
| 5. N. M. Greene     | 18. R. O. Sayer               |
| 6. K. Guber         | 19. M. S. Smith               |
| 7. J. A. Harvey     | 20. T. E. Valentine           |
| 8. J. N. Herndon    | 21. R. M. Westfall            |
| 9. D. J. Hill       | 22. RSICC                     |
| 10. C. M. Hopper    | 23. Central Research Library  |
| 11. H. T. Hunter    | 24. Laboratory Records - RC   |
| 12. D. T. Ingersoll | 25. Laboratory Records - OSTI |
| 13. B. L. Kirk      |                               |

## EXTERNAL DISTRIBUTION

26. P. Blaise, DER/SPRC/LEPH, Batiment 230, Centre dEtudes de CADARACHE, 13108 Saint Paul-lez-Durance, France
27. R. Block, Gaerttner LINAC Laboratory, Department of Environmental and Energy Engineering, Rensselaer Polytechnic Institute, Troy, NY 12180-3590
28. O. Bouland, DER/SPRC/LEPH, Batiment 230, Centre dEtudes de CADARACHE, 13108 Saint Paul-lez-Durance, France
29. D. E. Carlson, Reactor and Plant System Branch, Division of System Research, Office of Nuclear Regulatory Research, U.S. Nuclear Regulatory Commission, MS T-10 G6, RM T-10, I7, Washington, DC 20555-0001
30. R. F. Carlton, Department of Chemistry and Physics, Middle Tennessee State University, Murfreesboro, TN 37132
31. E. Caro, Lockheed Martin Corporation, P.O. Box 1072, Schenectady, N. Y. 12301-1072.
32. M. Chadwick, T-2, MS B243, Los Alamos National Laboratory, P. O. Box 1663, Los Alamos, NM 87545
33. D. H. Crandall, U.S. Department of Energy, NA-11, Washington, DC 20585

34. Y. Danon, Gaerttner LINAC Laboratory, Department of Environmental and Energy Engineering, Rensselaer Polytechnic Institute, Troy, NY 12180-3590
35. C. Dunford, Bldg 197D, National Nuclear Data Center, Brookhaven National Laboratory, Upton, NY 11973
36. P. Finck, Argonne National Laboratory, Reactor Analysis Division, Bldg 208, Argonne, IL 60439
37. E. Fort, DER/SPRC/LEPH, Batiment 230, Centre dEtudes de CADARACHE, 13108 Saint Paul-lez-Durance, France
38. C. M. Frankle, NIS-6, MS J562, Los Alamos National Laboratory, Los Alamos, NM 87545
39. F. Froehner, Kernforschungszentrum Karlsruhe, Institut fur Neutronenphysik und Reaktortechnik, Postfach 336 40, D-76021 Karlsruhe, Germany
40. S. Ganesan, Theoretical Physics Division, Central Complex, 5th Floor, Bhabha Atomic Research Centre, Trombay, Mumbai 400 085 INDIA
41. C. Gould, Physics Dept., North Carolina State University, Box 8202, Raleigh, NC 27695-8202
42. F. Gunsing, Centre DEtudes De Saclay, F-Saclay - 91191 GIF-SUR-YVETTE Cedex, France
43. G. M. Hale, MS B243 T-16 : NUCLEAR PHYSICS , Los Alamos National Laboratory, P. O. Box 1663, Los Alamos, NM 87545
44. A. Hasagawa, Nuclear Data Center, Japan Atomic Energy Research Institute, Tokaimura, Naka-gun, Ibaraki-ken 319-11, Japan
45. R. P. Jacqmin, DER/SPRC/LEPH, Batiment 230, Centre dEtudes de CADARACHE, 13108 Saint Paul-lez-Durance, France
46. N. Janeva, Bulgarian Academy of Sciences, 72, Boul, Tzarigradsko shosse, Sofia 1784, Bulgaria
47. G. Leinweber, Gaerttner LINAC Laboratory, Department of Environmental and Energy Engineering, Rensselaer Polytechnic Institute, Troy, NY 12180-3590
48. R. Little, X-CI, MS F663, Los Alamos National Laboratory, Los Alamos, NM 87545
49. C. Lubitz, Knolls Atomic Power Laboratory, P. O. Box 1072, Schenectady, NY 12301
50. R. E. MacFarlane, T-2, MS B243, Los Alamos National Laboratory, P. O. Box 1663, Los Alamos, NM 87545-1663
51. Alberto Mengoni, CERN, CH-1211, Geneva 23, Switzerland
52. C. Mounier, CEN Saclay, DMT/SERMA/LENR, 91191 Gif Sur Yvette Cedex, France

53. S. F. Mughabghab, Brookhaven National Laboratory, Advanced Technology, Building 197d, Upton, NY 11973-5000
54. C. Nordborg, OECD/NEA, Le Seine St-Germain 12, Boulevard Iles, 92130 Issy-les-Moulineaux, France
55. A. Nouri, OECD/NEA Data Bank, Le Seine Saint Germain, 12, Bd des Iles, 92130 Issy-Les-Moulineaux (France)
56. S. Y. Oh, Nuclear Data Evaluation Lab., Korea Atomic Energy Research Institute, P. O. Box 105, Yusung, Taejon, 305-600 South Korea
57. A. Plompen, Central Bureau for Nuclear Measurements, Steenweg op Retie, 2240 Geel, Belgium
58. A. Popov, Frank Laboratory of Neutron Physics, Joint Institute for Nuclear Research, RU-141980 Dubna, Moscow Region, Russia
59. C. Raepsaet, DSM/DRECAM/LPS, Bt637 Pce 107D, Centre d'tudes de Saclay, -91191 Gif-sur-Yvette Cedex, France
60. M. Salvatores, DRN/P, Batiment 707, C. E. CADARACHE, 13108 Saint Paul-lez-Durance, France
61. E. Sartori, OECD/NEA, Le Seine St-Germain 12, Boulevard Iles, 92130 Issy-les-Moulineaux, France
62. O. A. Shcherbakov, Petersburg Nuclear Physics Institute, 188 350 Gatchina, Leningrad District, Russia
63. R. Shelley, Central Bureau for Nuclear Measurements, Steenweg op Retie, 2240 Geel, Belgium
64. K. Shibata, Nuclear Data Center, Japan Atomic Energy Research Institute, Tokaimura, Naka-gun, Ibaraki-ken 319-11, Japan
65. P. Siegler, Central Bureau for Nuclear Measurements, Steenweg op Retie, 2240 Geel, Belgium
66. D. L. Smith, 1710 Avenida del Mundo No. 1506, Coronado, California 92118-3073
67. H. Takano, Nuclear Data Center, Japan Atomic Energy Research Institute, Tokaimura, Ibaraki-ken 319-11, Japan
68. C. Wagemans, Central Bureau for Nuclear Measurements, Steenweg op Retie, 2240 Geel, Belgium
69. J. J. Wagschal, Racah Institute of Physics, The Hebrew University of Jerusalem, 91904, Jerusalem, ISRAEL
70. J. P. Weinman, Lockheed Martin Corporation, P.O. Box 1072, Schenectady, N. Y. 12301-1072

71. C. J. Werner, Los Alamos National Laboratory, Los Alamos, NM 87545
72. R. M. White, Lawrence Livermore National Laboratory, P. O. Box 808, Livermore, CA 94550
73. K. Yoo, Nuclear Data Evaluation Lab., Korea Atomic Energy Research Institute, P. O. Box 105, Yusung, Taejon, 305-600 Korea
74. P. G. Young, MS B243 T-16 : NUCLEAR PHYSICS, Los Alamos National Laboratory, P. O. Box 1663, Los Alamos, NM 87545